

# 1        **Sedimentary and Geomorphic evidence of Saharan megalakes: a synthesis**

2        Drake, N.A.<sup>1,2\*</sup>, Candy, I.<sup>3</sup>, Breeze, P.<sup>1</sup>, Armitage, S.J.<sup>3,4</sup>, Gasmi, N.<sup>5,6</sup>, Schwenninger, J.L.<sup>7</sup>, Peat  
3        D.<sup>7</sup> Manning, K.<sup>1</sup>

4        <sup>1</sup>Department of Geography, King's College, London, UK

5        <sup>2</sup>Department of Archaeology, Max Planck Institute for the Science of Human History, Jena,  
6        Germany

7        <sup>3</sup>Department of Geography, Royal Holloway, Egham, Surrey, UK

8        <sup>4</sup>SFF Centre for Early Sapiens Behaviour (SapienCE), University of Bergen, Post Box 7805,  
9        5020, Bergen, Norway

10       <sup>5</sup> Faculty of Letters and Human Sciences of Sousse, University of Sousse

11       <sup>6</sup> Le Laboratoire de Cartographie Géomorphologique des Milieux, des Environnements et  
12       des Dynamiques (CGMED), Université de Tunis

13       <sup>7</sup> Research Laboratory for Archaeology and the History of Art, School of Archaeology, Oxford  
14       University of Oxford, UK

15       \* Corresponding author at: Department of Geography, King's College, London, UK. Email:  
16       [nick.drake@kcl.ac.uk](mailto:nick.drake@kcl.ac.uk)

## 17 18       **Abstract**

19       It has long been recognised that the Sahara Desert contains sediment, landform and  
20       palaeoecological evidence for phases of increased humidity during the Quaternary period.  
21       Many authors have also suggested that during some of these humid periods very large  
22       lakes, termed megalakes, developed in several basins within the Sahara. Recent work has  
23       questioned their existence. In particular it has been argued that the lack of well-developed  
24       and spatially extensive shorelines in these basins suggests that discrete groundwater and  
25       spring deposits have been misinterpreted as evidence for megalakes. In this paper we re-  
26       evaluate the evidence used to identify megalakes. Firstly, we apply a comprehensive remote  
27       sensing and GIS analyses to the megalake shorelines, their catchments and the wider  
28       Sahara. This not only supports the previously proposed existence of numerous megalakes,  
29       but also indicates a previously unrecognised megalake in the Niger Inland Delta region, here  
30       named Megalake Timbuktu. Secondly, we review the geomorphic and sedimentary evidence  
31       for the megalakes, highlighting the importance of the sedimentary record in identifying lake  
32       highstands, particularly through the example of the Chotts Megalake in southern Tunisia

33 where we provide new sedimentary information on lake shorelines. This analysis  
34 demonstrates that in much of the Sahara the dynamic aeolian systems preclude the  
35 preservation of well-developed shorelines, but the distribution of fragmented geomorphic  
36 features and localised lake deposits provide robust evidence for Quaternary megalake  
37 formation. The paper concludes by highlighting that although extensive evidence for  
38 Saharan megalake formation exists the current chronology of lake highstands indicates that  
39 the vast majority date to Marine Isotope Stage (MIS) 5 or earlier. Only megalakes Chad and  
40 Timbuktu, which derive much of their water from outside the desert, show evidence for  
41 Holocene (African Humid Period or AHP) shorelines. The AHP record of the other megalakes  
42 indicate the existence of much smaller water bodies than those that developed earlier in the  
43 Pleistocene indicating that it was significantly drier than these earlier humid phases.

#### 44 **Keywords**

45 **Sahara Desert; megalake; remote sensing and DEM analysis; sedimentology; shorelines.**

46

#### 47 **1. Introduction**

48 The Quaternary climate history of the low latitudes is dominated by cyclic changes in  
49 precipitation regime (Kutzbach and Street-Perrot, 1985; de Menocal et al., 2001; Prell and  
50 Kutzbach 1987). In multiple climate archives from these regions the timing of episodes of  
51 increased rainfall corresponds with precession modulated insolation maxima (Prell and  
52 Kutzbach 1987). This is seen most clearly in the  $\delta^{18}\text{O}$  signal of speleothems and in the  
53 dust/mineralogical composition of marine sequences of these regions (de Menocal et al.,  
54 2001; Vaks et al., 2010; Helmke et al., 2008; Meckler et al., 2012; El-Shenawy et al., 2018). In  
55 arid regions, such as the Saharan and Arabian deserts, the poor-preservation of traditional  
56 biological proxies, e.g. pollen, and the restricted growth of speleothems means that an  
57 understanding of long-term changes in relative humidity/aridity is strongly reliant on  
58 geomorphic and sedimentary evidence (Drake and Bristow, 2006; Bristow and Armitage,  
59 2016; Drake and Breeze, 2016). In areas that are currently arid/hyper-arid the presence of  
60 sediment/landform features such as spring mounds, travertine/tufa, lake shorelines,  
61 lacustrine sediments and fluvial deposits all provide evidence for hydrological processes  
62 being more active in the past (Grove and Warren, 1968; Kropelin et al., 2008). The dating of

63 these features by <sup>14</sup>C, luminescence techniques and U/Th disequilibria, allows the timing of  
64 these humid phases to be reconstructed (Causse et al., 1989; Armitage et al., 2015).

65 In areas such as the Sahara the existence of such evidence, and the concomitant  
66 implications for the occurrence of Quaternary “humid” phases, has long been acknowledged  
67 (Grove and Warren, 1968; Kuper and Kropelin, 2006; Kropelin et al., 2008; Drake et al.,  
68 2011). However, it is increasingly recognised that in some humid phases, the terrestrial  
69 record indicates that the landscape of the Sahara was not characterised by the existence of  
70 isolated and small-scale water bodies. Instead the record has been interpreted as indicating  
71 the existence of regional-scale integrated hydrological networks that occurred across the  
72 Sahara, terminating in a series of megalakes; megalakes Chad (Armitage et al., 2015; Drake  
73 and Bristow, 2006), Chotts (Causse et al., 1988; 1989; 2003; Zouari et al., 1998), Fezzan  
74 (Thiedig et al., 2000; Geyh and Thiedig 2008; Armitage et al., 2007; Drake et al., 2008),  
75 Darfur (Ghoneim and El-Baz, 2007); White Nile (Barrows et al., 2014; Williams et al., 2003),  
76 Tushka (Maxwell et al., 2010) and Ahnet-Mouydir (Conrad, 1970; Conrad and Lappartient  
77 1991; Drake *et al.*, 2011). The proposed existence of these megalakes has wide-ranging  
78 implications for both palaeoclimate, as their formation requires large-scale increases in  
79 mean annual precipitation, and human dispersal, as it has been suggested that in concert  
80 they acted as humid corridors across the desert aiding human migration (Drake et al., 2011;  
81 Drake et al., 2008).

82 Although the formation of Saharan megalakes (here defined as lakes > 25,000 km<sup>2</sup> in area)  
83 has been widely accepted, the evidence that supports this theory is spread across large  
84 numbers of articles published over many decades. As such, no detailed synthesis and state  
85 of the art review of the evidence underlying the proposed occurrence of Saharan megalakes  
86 currently exists. Such ambiguity led Quade et al., (2018) to query the existence of these  
87 water bodies, arguing instead that humid phases in the Sahara were characterised by  
88 discrete, small-scale, isolated wetlands. Their study used two main lines of argument. Firstly,  
89 they question the quality of the geological data used to infer the existence of megalakes.  
90 Quade et al., (2018) have interpreted remote sensing imagery and reviewed some of the  
91 literature on selected megalakes to suggest that the evidence for megalake shorelines is  
92 limited and that many of the sediments and landforms previously defined as lacustrine were  
93 in fact spring and ground water features. Secondly, Quade et al., (2018) argue that rainfall

94 within their mapped catchments of these megalakes was insufficient to generate surface  
95 water bodies of the extent that has been previously suggested. The re-interpretations by  
96 Quade et al., (2018) would have major implications for our understanding of both the  
97 Quaternary palaeoclimatic history of the region, and human dispersal pathways.

98 In this paper we re-evaluate Saharan megalakes in three different ways. Firstly, we  
99 investigate each of the proposed megalakes using a diverse array of remote sensing imagery  
100 compiled and viewed using Google Earth Engine (GEE) to allow seamless examination of the  
101 entirety of the Sahara. These data comprised PALSAR L band HH and HV radar, Landsat TM,  
102 Sentinel 2 and Google Earth imagery, Shuttle Radar Topography Mission (SRTM) and  
103 Advanced Land Observing Satellite (ALOS) 30 m Digital Elevation Model (DEM) data, in the  
104 form of global image mosaics which can be compared at the click of a button. Using these  
105 data we investigated all megalake basins, but also other large topographic basins in the  
106 Sahara where megalakes could have occurred. We first looked at known shorelines to  
107 evaluate the utility of the different types of imagery for lake shoreline identification. We  
108 then used this knowledge to survey all basins. This analysis identified previously  
109 unrecognised shorelines as well as evidence for a hitherto unacknowledged megalake in the  
110 Niger Inland Delta region of Mali, the evidence for which we present below. The  
111 interpretation of DEMs and satellite imagery can be subjective, leading to disagreements  
112 about the evidence for the existence of some megalakes. To provide greater clarity on the  
113 existence of megalakes we have developed a method that allows the interpreter to obtain  
114 different levels of confidence about the evidence for the presence of a lake in a basin during  
115 the past. We then apply this technique to all proposed megalakes to evaluate the veracity of  
116 the evidence for their presence.

117 Secondly, we comprehensively review the evidence for Saharan megalakes, using the  
118 criticisms from Quade et al., (2018) as a basis for discussion. This study focusses particularly  
119 on Megalakes Chad, Fezzan and Chotts, since these are the systems that the authors of this  
120 study have worked on directly. We also consider the newly discovered megalake Timbuktu  
121 as well as Megalakes White Nile, Tushka, Darfur and Ahnet-Mouydir, of which only the latter  
122 two were considered by Quade et al. (2018). Finally, when considering megalake Chotts we  
123 present new sedimentological information from shoreline sediments that provide evidence  
124 for the existence of a large water body.

125 The article begins by briefly summarising the history of research on Saharan megalakes and  
126 presents our current understanding of the major palaeo-water bodies in this region. The  
127 paper is then divided into two sections. Firstly, the geomorphic and sedimentary evidence  
128 for megalakes is reviewed and new results presented that not only confirms the existence of  
129 most megalakes, but also reveals a new one along the Niger River in Mali. Secondly, the  
130 mapping of megalake catchments and the modelling of water levels is summarised and  
131 discussed. The paper continues by arguing that robust evidence exists for the occurrence of  
132 megalakes in the Sahara, in contrast to prior assertions by Quade et al., (2018). This study  
133 concludes by emphasising that although the vast majority of basins contain abundant  
134 evidence for the occurrence of megalakes, their chronology is often poorly constrained. This  
135 has significant implications for interpreting the Quaternary history of the Saharan region  
136 and the associated archaeological record.

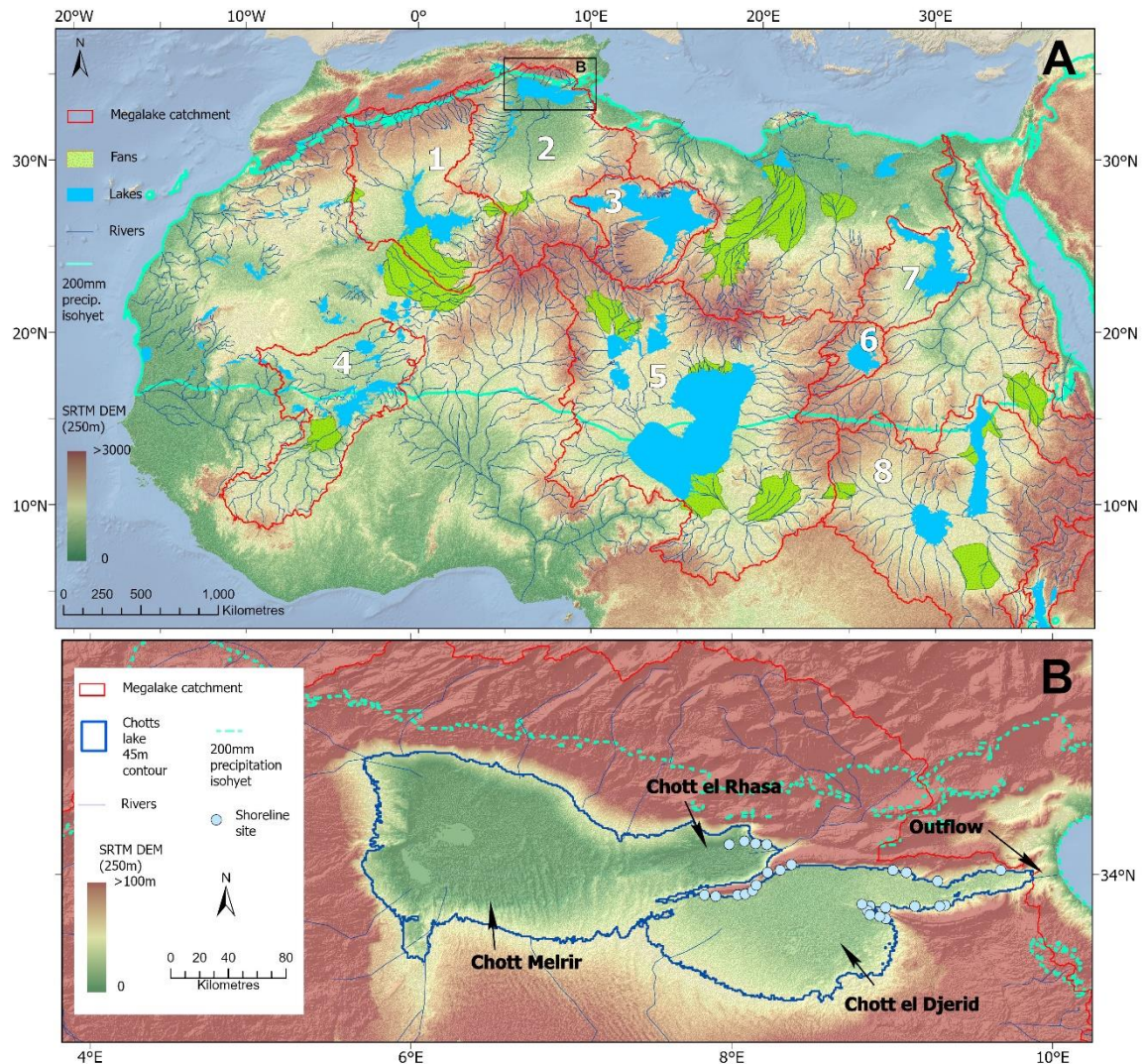
## 137 **2. Mega-Lakes in The Sahara – Current Ideas and Understanding**

138 Evidence for increased surface water in the Sahara during different periods within the  
139 Quaternary has been recorded by large numbers of studies utilising a diverse range of  
140 evidence (Goudie, 1992; Kutzbach and Street-Perrot, 1985; Kuper and Kropelin, 2006).  
141 Whilst much of this evidence could indicate the existence of localised and discrete wetland  
142 environments or spring systems, some of it has been used to suggest the existence of large  
143 lake systems, or megalakes, that if existing reconstructions are correct (Figure 1A), would  
144 range in extent from 27,000 km<sup>2</sup> (megalake Timbuktu) to 361,000 km<sup>2</sup> (megalake Chad;  
145 Drake and Bristow 2006).

### 146 *2.1 Megalake Chad*

147 Megalake Chad (Figure 1A) is the largest of the systems discussed here and has an extensive  
148 network of shoreline features, identifiable by a range of techniques (e.g. Drake and Bristow  
149 2006; Schuster et al., 2005). These include evidence for palaeo-shorelines eroded into the  
150 landscape, littoral sediment accumulations (deltas, spits and berms, Drake and Bristow,  
151 2006) and fine-grained deposits within the deeper parts of the basin that contain diatoms  
152 (Gasse, 2002), ostracoda and molluscs (Bristow *et al.*, 2018) indicative of freshwater  
153 conditions. Dating of numerous shorelines suggest megalake Chad existed between 5-11 ka  
154 (Armitage et al., 2015) and during MIS5, with two beach ridges dated to 114.2±14 and

155 125.4±11.6 ka (Drake et al., 2011). The evidence preserved in the Chad basin is, therefore,  
 156 extensive and well-documented. Consequently, it is only megalake Chad, of all the proposed  
 157 Saharan megalakes, that Quade et al., (2018) support the existence of.



158  
 159 Figure 1. A) Map showing the topography (SRTM 1 km DEM) of North Africa overlain with the  
 160 present-day 200 mm isohyet as defined by Worldclim (Fick and Hijmans, 2017), the location of the  
 161 main rivers, fluvial fans, paleolakes, the catchments of the megalakes and their extent (from Drake  
 162 et al., 2011 with new data added). 1 Ahnet-Mouydir, 2 Chotts, 3 Fezzan, 4 Timbuktu, 5 Chad, 6  
 163 Darfur, 7 Tushka, 8 White Nile. B) Megalake Chotts topography (SRTM 30 m DEM) overlain with  
 164 rivers, megalake catchment boundary, present-day 200 mm isohyet and the 45 m contour, around  
 165 which the location of the 27 shoreline sites (light blue dots) reported by Coque (1962) are clustered.

166  
 167

## 168 2.2 Megalake Chotts

169 Megalake Chotts (Figure 1A) is one of the smallest of the proposed megalake systems  
170 (~30,000 km<sup>2</sup>) and is comprised of three sub-basins (Figure 1B), Chott el Djerid, Chott  
171 Melrhir and Chott el Rhasa which span southern Tunisia and eastern Algeria (Coque, 1962;  
172 Richards and Vita-Finzi, 1982; Causse et al., 1989; Zouari et al., 1998). The identification of  
173 this megalake is heavily reliant on the occurrence of outcrops of shell rich sediments that  
174 have been interpreted as littoral lacustrine deposits (Figure 1B). These occur at an altitude  
175 of about 45 m over distances of 150 km around the margins of the Chotts el Djerid and el  
176 Rhasa, but are most abundant around the northern margin of Chott el Djerid near the  
177 Tunisian town of Touzeur (Coque, 1962; Causse et al., 1989; Zouari et al., 1998). The  
178 dominant shells within these sediments are of the species *Cerasteroderma glaucum*.  
179 Although classed as a brackish water species, *C. glaucum* is tolerant of a range of salinities  
180 and is found in lagoons on the coast of Tunisia today. Consequently, some early researchers  
181 ascribed the formation of these deposits, which are rich in brackish-water indicators, to a  
182 marine environment prior to a phase of uplift (Richards and Vita-Finzi, 1982). However,  
183 since it is now widely accepted that there has been no recent (since the Plio-Pleistocene)  
184 marine incursion, the *C. glaucum* deposits are today interpreted as lake shoreline sediments  
185 (Causse et al., 1988; 2003; Zouari et al., 1998). These deposits do not form a well-defined  
186 continuous shoreline (Causse et al., 1988; Zouari et al., 1998), but they are found at the  
187 same altitude (~45m), and this corresponds with that of the low point of the Chott el Djerid  
188 sub-basin watershed, through which a lake would overflow into the Mediterranean Sea near  
189 the town of Gabes (Figure 1B). At ~45 m the spillways separating Chott sub-basins would  
190 also be overtopped, generating a single extensive water body.

## 191 2.3 Lake Megafezzan

192 The Fezzan basin is located in western Libya and contains extensive evidence for large-scale  
193 lake development during the Neogene. This evidence consists of extensive limestone beds  
194 that are distributed throughout much of the basin. When their distribution is considered in  
195 relation to the topography of the basin it suggests a maximum lake area of 135,000 km<sup>2</sup>  
196 (Drake et al., 2008). There has been much debate about the timing of lake high-stands in the  
197 Fezzan. Thiedig et al., (2000) and Geyh and Thiedig (2008) argued that the lakes were  
198 Middle Pleistocene, probably MIS 7 and 11, based on U/Th dating of limestones. Brooks et



199 al., (2003) proposed a lake highstand during the Holocene AHP based on identification of a  
200 shoreline, while Armitage et al., (2007) used luminescence dating of this shoreline along  
201 with sub-aqueous lake sediments to suggest high stands during the AHP and MIS 11. Drake  
202 et al., (2008) re-assessed the geomorphology of the proposed Holocene shoreline and  
203 concluded that it was in fact a springline, thus refuting a Holocene age for Lake Megafezzan.  
204 They investigated the sedimentology of the limestone bed reported in Geyh and Thiedig  
205 (2008) concluding that numerous thick sections (up to 30 m) of superimposed sand and  
206 limestone units indicated multiple, discrete lacustrine cycles. Hounslow et al., (2017)  
207 investigated similar sedimentary sections throughout much of the Fezzan Basin, and showed  
208 that their stratigraphy can be correlated over vast distances. Magnetostratigraphy of these  
209 sediments demonstrates that numerous high-stands occurred during the Miocene  
210 (Hounslow et al., 2017). Younger lake sediments in the basin yield MIS5 and Holocene ages  
211 (Drake et al., 2018), though in both cases these lakes were much smaller features (maximum  
212 surface area of  $\sim 1600\text{km}^2$ ) than the megalake phases recorded in the Miocene limestone  
213 deposits. The evidence for these Late Pleistocene lake stands consists of birdsfoot deltas,  
214 coquinas and shell rich sands that contain sedimentary structures consistent with wave  
215 action and delta progradation at a lake margin (Drake et al., 2018). These deposits are  
216 interpreted by Quade et al., (2018) as spring deposits, however the presence of deltas and  
217 the evidence for wave action clearly precludes this possibility.

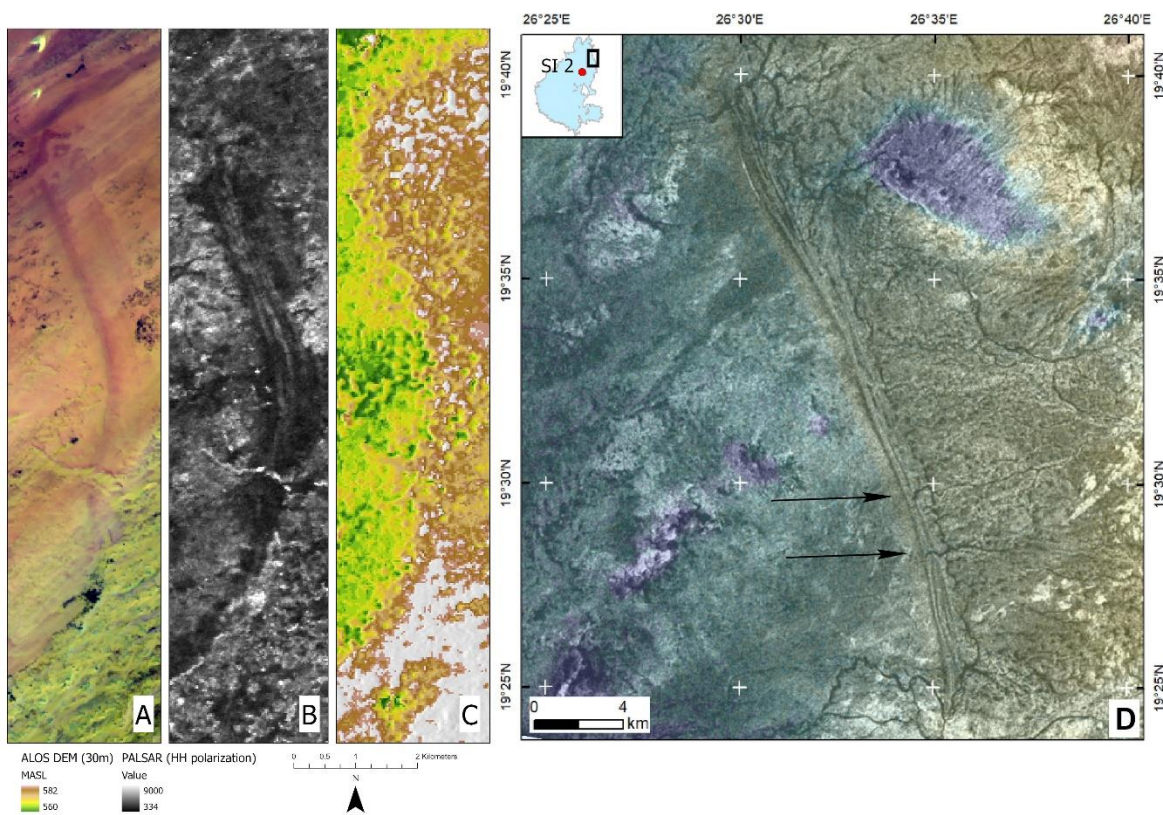
218

#### 219 *2.4 Megalake Darfur*

220 In Darfur, Ghoneim and El-Baz (2008) record the presence of shoreline features, the most  
221 impressive of which comprises multiple beach ridges that are stacked against each other  
222 (Figure 2D). These beach ridges occur at the height of an overflow spillway ( $573\pm 3$  m),  
223 strongly implying that they were formed by an extensive water body within the Darfur  
224 basin. The beach ridges are neither extensive nor continuous, but their form and altitude is  
225 consistent with formation by a megalake. The altitude of the implied shoreline indicates that  
226 it had an area of  $30,750\text{ km}^2$ . The age of this feature is currently poorly constrained,  
227 although Szabo et al. (1995) provided U-series estimates for a number of marl deposits in  
228 the region. Whilst some of these yielded early Holocene ages, implying the existence of  
229 water bodies during the AHP, the majority of ages relate to Pleistocene humid phases,



230 including early and late MIS 5, MIS 7 and MIS 9. During the AHP there is evidence that a  
 231 smaller lake (about 5330 km<sup>2</sup>) existed in the Darfur basin (Hoelzmann et al., 2000). Since  
 232 Hoelzmann et al. (2000) identified no shorelines related to this lake, the approximate area  
 233 was determined using the elevation of archaeological settlements concentrated around the  
 234 lake margin at an altitude of 555 m. Interestingly, this is precisely the elevation that we  
 235 determine from the ALOS 30 m DEM for a shoreline beach ridge first identified by Parchur  
 236 and Rottinger (1997) using radar imagery. Thus, two independent forms of evidence  
 237 (remotely sensed and archaeological) suggest a lake shoreline at this altitude. Radiocarbon  
 238 dating of the lake sediments suggests it existed between 9 and 4 ka, whilst highly depleted  
 239 oxygen isotopes indicate intense summer rainfall, suggesting that the lake formed under an  
 240 enhanced monsoon (Hoelzmann et al., 2001). These Holocene lake sediments preserve Nile  
 241 Perch bones (Hoelzmann et al., 2001), a species that requires large (a minimum of several  
 242 km<sup>2</sup>), deep (several meters) and well oxygenated waterbodies (Van Neer 2012). The  
 243 presence of Nile Perch in the Darfur sediments is inconsistent with them being spring  
 244 deposits, as suggested by Quade et al., (2018).



245

246 Figure 2. Paleolake shoreline of Megalake Darfur as revealed by (A) Sentinel 2 bands 12, 8, 2 (RGB)  
 247 colour composite. The light north-south trending brown curvilinear feature is a beach ridge

248 shorelines. B) PALSAR HH polarisation radar image shows that the shoreline is composed of four  
249 ridges stacked against each other. C) the ALOS 30 m DEM showing the shoreline break of slope. D)  
250 Radarsat-1 image of the north-eastern part of the Megalake. In order to illustrate the topography,  
251 the SRTM 90 m DEM has been superimposed on the Radarsat-1 image with 85% transparency. A  
252 long palaeoshoreline showing beach ridges stacked against each other is evident. The two small  
253 wadis that are marked with arrows terminate exactly where they join the shoreline zone, as would  
254 be expected if they fed a paleolake and dried up at the same time it did (adapted from Ghoneim and  
255 El-Baz (2008)).

256

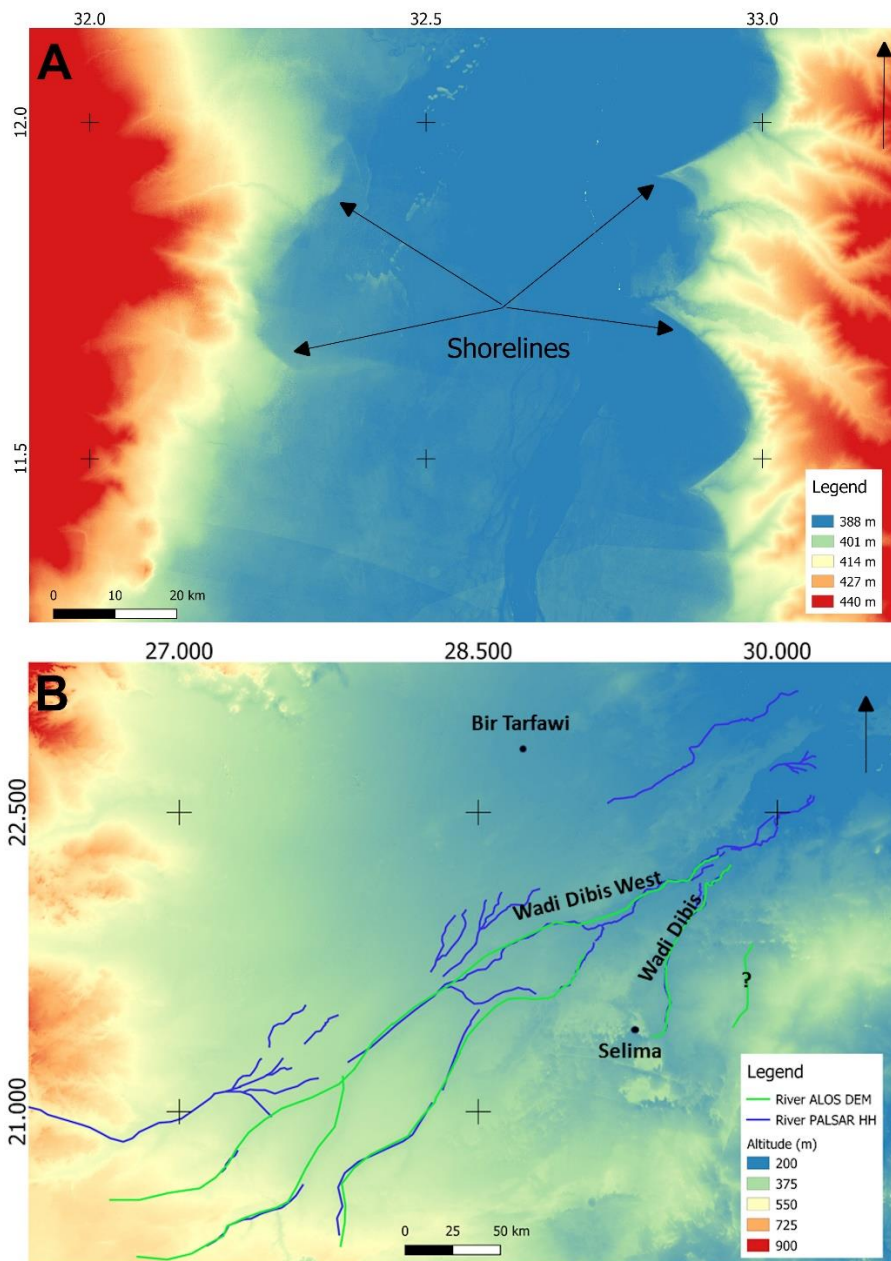
### 257 *2.5 Megalake Ahnet-Mouydir*

258 Conrad (1970) postulated the existence of a large lake in the Ahnet-Mouydir basin, based on  
259 extensive exposures of lake sediments. Causse et al., (1988) dated a substantial lake  
260 sediment outcrop using U/Th disequilibria to  $92 \pm 20 -18$  ka and Drake et al., (2011) used  
261 both the topography and altitude of the Causse et al., (1988) section to suggest that the  
262 Ahnet-Mouydir lake had a minimum surface area of  $\sim 50,000$  km<sup>2</sup>. Conrad and Lappartient  
263 (1991) summarise the geomorphology and sedimentology of the basin, reporting a number  
264 of locations with thick sections (up to 30 m) of lacustrine and deltaic sediments,  
265 characterised by a rich fauna of fresh and saline tolerant molluscs, ostracods, diatoms,  
266 foraminifera, and fish bones concentrated in several different levels. Such sediments could  
267 only have been deposited by an extensive lake.

### 268 *2.6 Megalakes along the River Nile*

269 Two megalake basins have been proposed along the course of the River Nile (Figure 1A). The  
270 first was identified on the basis of a shoreline adorned by cusped headlands, spits and  
271 embayments located on the eastern margin of the Nile Valley (Figure 3A) south of Khartoum  
272 (Williams et al., 2003). This shoreline lies at an elevation of 386 m and was formed by a lake  
273 with an area of 45,000 km<sup>2</sup> (Williams et al., 2003). Like megalake Chad, this lake was fed by  
274 headwaters outside the Sahara, and extended southwards into the Sahel (Figure 1A).  
275 Burrows et al., (2014) report a <sup>10</sup>Be age of  $109 \pm 8$  ka for the shoreline. Regional topography  
276 suggests that the lake was formed by an increase in White Nile discharge (Williams et al.,

277 2003), implying higher effective rainfall both locally and in the headwaters around Lake  
278 Victoria.



279

280 Figure 3. A) ALOS 30 DEM of the White Nile Megalake shorelines. The eastern shoreline is clearly  
281 evident in marked contrast to the western margin of the lake. The arrows indicate the only two  
282 fragments of the shoreline preserved on the western side of the lake and some of the most obvious  
283 shorelines on the eastern side, where similar features are preserved for much of its length (750 km).  
284 B) ALOS 30 m DEM of the Selima Sand Sheet. The rivers that were manually digitised from the DEM  
285 are shown in green whilst those digitized from the Palsar HH imagery are shown in blue.

286

287 The second proposed Nile megalake is located downstream of the first in northern Egypt.  
288 Maxwell et al., (2010) used SRTM 90 m DEM data to show that river channels flowing into a  
289 depression west of the Nile Valley terminate at an altitude of ~247 m. This altitude matches  
290 the elevation of Middle Pleistocene fish fossils at Bir Tarfawi, which is located in the same  
291 basin, suggesting that the channels terminated in a megalake of 68,200 km<sup>2</sup> in the basin  
292 (Maxwell et al., 2010). A lower lake level (190 m) is also postulated based on the elevation  
293 of Wadi Tushka, a river valley that links the River Nile to the basin. The elevation of this  
294 channel is consistent with Palaeolithic sites at Bir Kiseiba and Maxwell et al., (2010) use this  
295 evidence to suggest a further lake at this time. It is proposed that the source waters for both  
296 these lakes was local rainfall and the overflow of the Nile through Wadi Tushka during  
297 periods of strengthened monsoons.

298

### 299 **3. Saharan Megalakes – Myth or Reality?**

300 The existence of the Saharan Megalakes discussed above has recently been challenged by  
301 Quade et al., (2018) who examined remotely sensed data from the proposed megalake  
302 basins and suggest that no reliable evidence exists for well-developed and spatially  
303 extensive shorelines in these regions. They use their extensive experience of working on  
304 large lake systems from elsewhere in the world to suggest that any major lacustrine system  
305 would, on the basis of water depth and surface area, be affected by wave processes. These  
306 wave dominated shores should be characterised by the erosion of sediments and the  
307 deposition of shorelines composed of wave mobilised bodies of sediment. Such shorelines  
308 would also include deltaic landforms that represent sediment accumulation at the interface  
309 between the lake and major tributaries. Furthermore, they suggest that shorelines produced  
310 by these wave processes should be characterised by sedimentary evidence for wave activity  
311 (cross-bedding and rounded-clasts for example). The absence of such shoreline features has  
312 led Quade et al., (2018) to suggest that these megalakes cannot have existed, and that any  
313 lake deposits (e.g. marls, mudstones and gypsum) relate to much smaller, discrete wetland  
314 systems, whilst any “shoreline” deposits are likely to be spring or groundwater related  
315 features that have been misinterpreted as indicative of a more extensive lake system. To aid  
316 future researchers, Quade et al., (2018) propose a series of objective criteria for identifying  
317 ancient megalakes. However, despite their extensive field experience in other regions of the

318 world, the authors of this study do not appear to have visited any of the Saharan sites which  
319 they discuss. Instead, Quade et al., (2018) dismiss geomorphic evidence for the existence of  
320 Saharan megalakes based solely on interpretation of satellite imagery and their  
321 reinterpretation of published data. The second argument made by Quade et al., (2018) is  
322 that the volume of water required to generate the proposed megalakes is too great to be  
323 feasible given: 1) The extent of their reconstructed catchment of each system; 2) The  
324 modern annual rainfall regime at the location of each megalake (typically  $\ll 100 \text{ mm a}^{-1}$ ) and  
325 3) the modelled increase in mean annual rainfall in “wet” phases during the Holocene humid  
326 period, relative to present day rainfall.

327 The review by Quade et al., (2018) is important for two reasons. Firstly, it provides objective  
328 criteria for identifying ancient megalake systems. Secondly, it attempts to synthesise  
329 geomorphic data from a range of lake basins across the Sahara. This is the first exercise of  
330 its kind as most studies focus on reconstructions that are specific to individual basins.  
331 Because the findings of this work have major implications for both the palaeoclimate and  
332 human history of the Sahara, we discuss the ideas and issues raised by Quade et al. (2018) in  
333 the following sections. In the next section we consider the presence/absence of shoreline  
334 features in the landscape of the megalake basins and discuss the evidence for such features  
335 along with the possible causes for their absence. In the subsequent section we discuss the  
336 modelling of the catchments of these basins and the implications that this has for the  
337 viability of megalake formation.

338

#### 339 **4. Geomorphological and Sedimentary Evidence for Saharan Megalakes**

##### 340 *4.1 Geomorphic evidence for shoreline features*

341 A major tenet of the Quade et al., (2018) argument is that in the majority of the large lake  
342 systems that they have worked on, well-developed and spatially extensive shoreline  
343 features exist. They provide a number of examples, including Lake Bonneville (North  
344 America), Lake Lisan (Middle East), Ngangla Ring Tso (Asia), Lake Uyuni and Cardiel (both  
345 South America) which have mappable and readily identifiable shoreline landforms. A key  
346 difference between the large lake systems described by Quade et al., (2018) and the  
347 Saharan lake systems is the far greater importance of aeolian processes in the latter

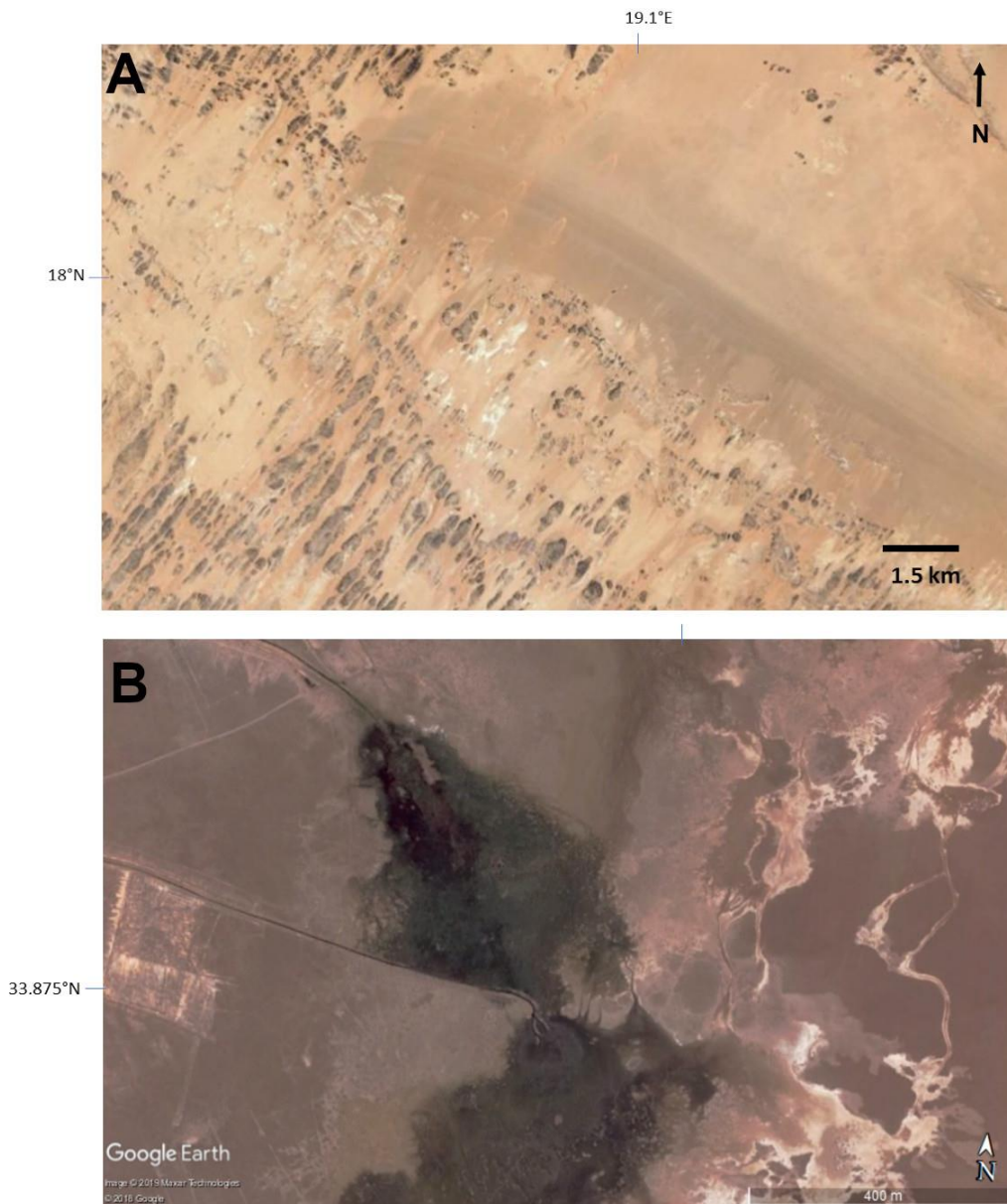
348 (Sweezey, 2003). In much of the Sahara, and in particular in the proposed megalake basins,  
349 aeolian erosion and deposition is a major geomorphic process, and active sand sheets and  
350 dune systems cover a significant proportion of all of these basins. For example, ~55% of the  
351 megalake Darfur catchment is covered by sand (Hoelzmann et al., 2000), with the majority  
352 of these deposits being found in the centre of the basin where they largely obscure lake  
353 sediment and shoreline exposures. Dune fields are particularly common in these low lying  
354 areas because rivers transport sands and other fine grained sediments to these regions  
355 during humid periods and they are subsequently reworked during arid episodes.

356 Aeolian processes have the ability both to erode and to bury shoreline features. The  
357 effectiveness of such processes is amplified by the fact that the Saharan shoreline deposits  
358 are, in our experience, comprised primarily of sand and are therefore highly susceptible to  
359 aeolian erosion. In contrast, the examples cited by Quade et al., (2018) occur in regions  
360 where dune fields are negligible. It is likely that aeolian processes are key to the sediment  
361 dynamics of these Saharan megalake systems. Aeolian sands mobilised during arid phases  
362 and stabilised at the transition into more humid phases may subsequently be remobilised by  
363 lake processes and redeposited as shoreline features. These features are then eroded and  
364 reworked by the wind during the following arid phase. This process is clearly shown in  
365 Figure 4A, where the main shoreline of megalake Chad can be seen to terminate as it enters  
366 a sand transport corridor where wind is funnelled between the Ennedi and Tibetsi  
367 Mountains (Washington et al., 2006). Strong winds have eroded any trace of the shoreline  
368 for the next 100 km to the north and west.

369 Those shorelines that are not subject to aeolian erosion may instead be buried by  
370 transported sand. For example, as 55% of the Darfur basin is covered by sand, it would be  
371 expected to obscure substantial portions of any shoreline features which are present.  
372 Similarly, within the proposed Chotts megalake system, deflation of the Chott el Djerid  
373 saline mudflats produces a considerable amount of gypsum sand which is transported in a  
374 south-westerly direction and deposited on the south-western margin of the depression  
375 (Drake, 1997). This gypsum dunefield covers approximately one quarter of the proposed  
376 Chotts Megalake shoreline. Whilst Quade et al., (2018) propose that contiguous shoreline  
377 preservation is a pre-requisite for the identification of megalake highstands, we argue that  
378 aeolian sediment dynamics make this criterion unsuitable for application in the Sahara.



379 Instead we propose that the intermittent preservation or indeed complete absence of  
380 shoreline features is likely to be characteristic of regions such as the Sahara.



381  
382 Figure 4. A) Bing Maps image of the termination of a megalake Chad AHP beach ridge (Microsoft  
383 product screen shot reprinted with permission from Microsoft Corporation). B) Google Earth image  
384 of the region between the Tozeur Oasis and the Chott el Djerid, showing wastewater drainage  
385 channels and plumes of water dispersing across the mudflat where they terminate. The straight dark  
386 lines feeding the water plumes are channels dug into the saline mudflats of the Chott el Djerid in  
387 order to dispose of excess irrigation water from Tozeur oasis. These plumes were identified as  
388 springs by Quade et al., (2018). However, these are anthropogenic features (Imagery, Google, Maxar  
389 Technologies 2019).



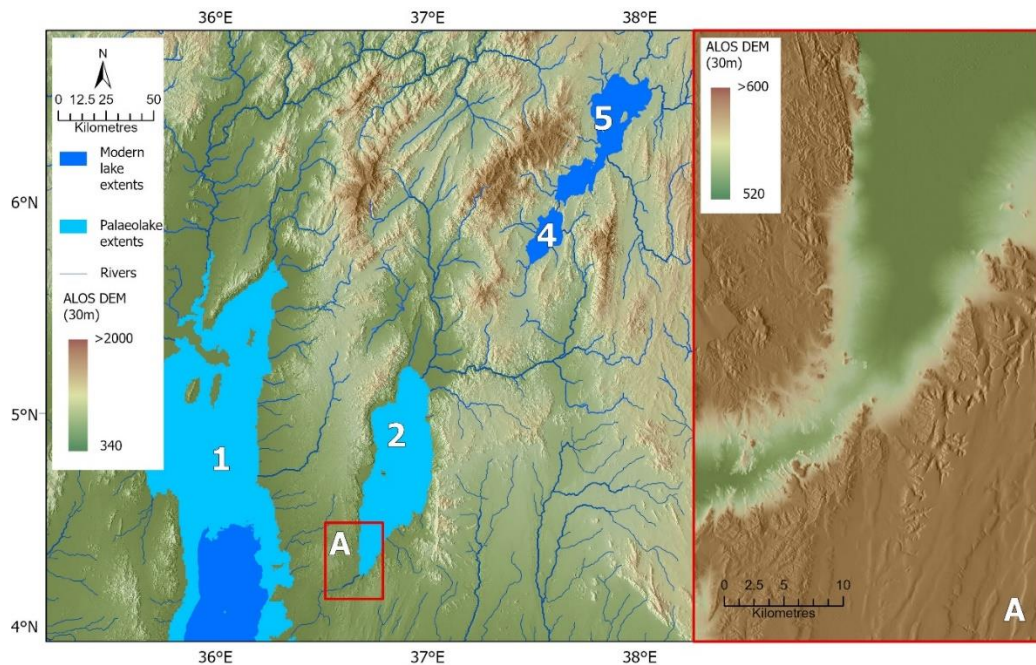
390

391 Regardless of the role aeolian processes play in shoreline preservation, the assertion by  
392 Quade et al., (2018) that all lakes produce well-developed shorelines does not appear to  
393 hold. For example, in Ethiopia and Kenya at the southern end of the Main Ethiopian Rift  
394 there are three large endorheic basins containing Lake Abaya (surface area 1,081 km<sup>2</sup>), Lake  
395 Chamo (310 km<sup>2</sup>) and paleo-lake Chew Bahir. The latter is now a 210 km<sup>2</sup> saline mudflat  
396 (Fischer et al., 2020), but in the middle of last century it was a lake with an area of 2,200 km<sup>2</sup>  
397 (Figure 5). During the AHP these lakes were much larger and deeper than they are today, as  
398 evidenced by paleochannels linking Lake Abaya to Chamo (18 m above its present lake  
399 level), Chamo to Chew Bahir (14 m above the modern lake) and Chew Bahir to Lake Turkana  
400 (45 m above the now dry basin floor; Fischer et al., 2020). Analysis of cores from Chew Bahir  
401 indicates that a lake high-stand lasted throughout much of the AHP (Foerster et al., 2012).  
402 When this was the case the Abaya-Chamo-Chew Bahir-Turkana lake cascade system was  
403 functioning and all these lake were full. Given their large surface area, volume, and the  
404 duration of the high stand, one would expect to find palaeoshorelines in the basin,  
405 particularly at the altitude of the outflow channels. However, investigation of satellite  
406 imagery (PALSAR, Landsat TM, Sentinel 2 and Google Earth) and the ALOS 30 m DEM shows  
407 none are evident (Figure 5 A and B). Indeed, the only reported evidence for lake high stands  
408 that have been found found at Chew Bahir, are scattered shell beds found at the same  
409 elevation as the overflow sill (Fischer et al., 2020). This analysis demonstrates that not all  
410 large lakes produce shorelines that are clearly visible in satellite imagery or DEMs, and  
411 sometimes they only leave behind a small amount of scattered sedimentological evidence.

412

413 The absence of well-defined shorelines, even in areas where aeolian processes do not  
414 dominate, could reflect a number of factors. Firstly, to produce a well-developed shoreline  
415 feature, wave energy must be focussed at a tightly defined location for a substantial period  
416 of time. However, if the lake level and therefore the location of the shoreline routinely  
417 fluctuated, the result would be that any associated erosion/deposition would have been  
418 “smeared” across a broad area. This is likely to be particularly true in regions where the  
419 landscape surrounding the lake is subdued with a low gradient. In such settings, small  
420 changes in the altitude of the lake water will shift the focus of shoreline erosion/deposition

421 to a different location, again resulting in sediments and landforms being spread over wide  
 422 areas. Modern Lake Chad provides an example of such a lake and has not produced well-  
 423 developed shoreline geomorphology during the last 3 ka. Secondly, if the underlying  
 424 bedrock is soft and mechanically unresistant, as is the case in many of the Saharan megalake  
 425 basins discussed here, then any geomorphic features cut into it are easily erodible. This  
 426 means that even where erosive shoreline features are formed, they can subsequently be  
 427 readily erased from the landscape and have limited preservation potential. These factors,  
 428 combined with the impact of aeolian processes, may mean that many large lake systems  
 429 leave patchy evidence for shoreline features in the landscape, even after prolonged high  
 430 stands.



431  
 432 Figure 5. Topography of the Chew Bahir catchment and the northern part of the Lake Turkana as  
 433 revealed by the ALOS 30 m DEM. Rivers are derived from HydroSHEDS and calculated using  $>100 \text{ km}^2$   
 434 in upstream accumulation area (Lehner et al., 2008). Current lake extent was obtained from the  
 435 Global Water Occurrence dataset (Pekel et al., 2016, thresholded to areas with water  $> 90\%$  of the  
 436 time between 1984 and 2015), and paleolake extents from Drake et al., (2011). 1) Lake Turkana, 2)  
 437 Paleolake Chew Bahir, 3) Lake Chamo and 4) Lake Abaya. The red box (A) outlines the outflow  
 438 channel of Paleolake Chew Bahir that is shown in more detail on the right.

439

440 *4.2 Remote sensing and DEM analysis of shoreline features*

441 Many Saharan megalakes have been identified through detection of shorelines (e.g.  
442 megalake Chad and Timbuktu) or shoreline fragments (e.g. megalake Darfur and White Nile)  
443 using DEMs (e.g. Drake and Bristow 2006) or different types of remote sensing imagery  
444 including radar (Ghoneim and El-Baz 2008) and visible and infrared (Barrows et al., 2014).  
445 However, it is unclear what types of imagery or DEMs are best employed to implement a  
446 systematic analysis of megalake shorelines. In order to answer this question we investigated  
447 known shoreline using all the different types of satellite imagery and DEMs outlined in  
448 section 1. We found that the ALOS 30 m DEM identified all shorelines while the SRTM 30 m  
449 DEM identified fewer because it exhibited more noise and contained many areas with no  
450 data, since strong absorption of the radar energy precluded altitude estimation. PALSAR HH  
451 radar imagery identified many shorelines and, in some cases, added extra detail (e.g. Figure  
452 2A, B and C). In contrast PALSAR HV imagery was extremely poor for shoreline detection.  
453 Visible and infrared imagery was approximately as effective as PALSAR HH imagery, and  
454 commonly provided detail not evident in the ALOS 30 m DEM or the radar imagery. Typically  
455 visible and infrared imagery was most useful where shoreline topography caused vegetation  
456 patterning and became more effective with higher spatial resolution (i.e. Google Earth  
457 imagery was more effective than Sentinel 2, which in turn was more effective than Landsat  
458 TM). Given these findings, our systematic mapping of shorelines started with ALOS. Once an  
459 interesting feature was detected the other types of imagery were studied to see if they  
460 provided further information to confirm or refute shoreline identification. The findings of  
461 this image interpretation are outlined below, where they are integrated with the wider  
462 literature on megalake geomorphology.

463

#### 464 *4.3 Evaluation of Megalake Geomorphology*

##### 465 *4.3.1 Megalake Chad and Darfur*

466 Quade et al., (2018) accept that the Chad basin contains a number of megalake shorelines,  
467 but dismiss the identification of shorelines in the Darfur basin on the basis that they are  
468 insufficiently extensive and have not been validated by field observations. However, Quade  
469 et al., (2018) do not discuss the most obvious shorelines in the Darfur basin, despite  
470 Ghoneim and El-Baz (2008) identifying multiple beach ridges stacked against each other

471 (Figure 2D). Furthermore, Ghoneim and El-Baz (2008) present compelling circumstantial  
472 evidence that the Darfur shorelines delimit a large lake. Firstly, multiple shorelines are  
473 preserved at the same elevation as the lowest point in the catchment perimeter, suggesting  
474 that the altitude of highstands was controlled by the elevation of a lake overflow. Secondly,  
475 two small wadis that flow into the Darfur basin have cut distinct channels into the  
476 surrounding landscape, but both channels terminate at the elevation of the proposed  
477 shorelines (Figure 2D). This landform arrangement is typical of rivers flowing into an  
478 extensive lake basin and grading to that regional base-level. Our analysis of the megalake  
479 using the Sentinel-2 20 m imagery, the ALOS 30 m DEM and the 25 m resolution PALSAR HH  
480 radar imagery has identified further shorelines landforms at the same altitude, including a  
481 series of beach ridges (Figure 2A, B and C) that are preserved at the same elevation as the  
482 shorelines shown in Figure 2D. These landforms could not have been formed by anything  
483 other than a lake. The fact that the shorelines associated with megalake Darfur are sparse  
484 and poorly preserved is consistent with the impact of aeolian processes described above.

#### 485 *4.3.2 Megalakes along the River Nile*

486 The proposed White Nile megalake shoreline is poorly preserved. The ALOS DEM reveals a  
487 370 km long stretch of well-developed shoreline on the eastern shore, but only two  
488 fragments on the western shore (Figure 3A) and nothing at the northern and southern  
489 margins. Shorelines are not evident on alluvial fans, where sand dunes are present, or when  
490 the shoreline is close to the active channel of the River Nile. These observations imply that  
491 most of the shoreline has been obliterated by a combination of aeolian and fluvial activity.  
492 Fluvial activity is particularly important in erasing geomorphic evidence for the White Nile  
493 megalake, since it extends outside the Sahara into the more humid Sahel.

494 We have reanalysed portions of the White Nile megalake shoreline using the ALOS 30 m  
495 DEM in a geographical information system (GIS) and find it to be about 10 m higher than  
496 reported by Williams et al., (2003) and Burrows et al., (2014). The preserved shoreline is no  
497 longer flat, being 9 m higher in the south than it is in the north, making lake area estimation  
498 difficult. Based on the mean shoreline height we calculate the lake area to have been 70,660  
499 km<sup>2</sup>, substantially larger than previous estimates. Below the main shoreline there is a bench,  
500 5 m above the present-day river level at an elevation of 382 m, which has been interpreted  
501 as a further lake shoreline (Williams et al 2003). This shoreline has been dated to the late

502 Pleistocene and early Holocene, when White Nile flooding formed a lake with an area of  
503 4690 km<sup>2</sup> (Williams et al., 2006).

504 The Tushka megalake is unique amongst proposed Saharan megalakes, since it was  
505 identified on the basis of fluvial rather than lacustrine landforms, and no shorelines have  
506 been reported. Maxwell et al., (2010) used the SRTM 90 m DEM to show that three wadis in  
507 the Tushka basin all terminate at the same elevation as lake sediments at Bir Tarfawi.  
508 However, few other outcrops of lake sediment are found in the basin that can be directly  
509 attributed to this lake, whilst the Bir Tarfawi sediments have since been shown to have been  
510 formed by a much smaller lake (Hill and Schild 2017). Furthermore, our analysis of the ALOS  
511 DEM shows that the three wadis studied by Maxwell et al., (2010) cease to be visible in the  
512 DEM at different altitudes (241 m (Wadi Dibis), 224 m (Wadi Dibis West) and 299 m (the  
513 wadi marked with a question mark in Figure 2 of Maxwell et al., 2010 and in Figure 3B),  
514 rather than 247 m as Maxwell et al. (2010) proposed. Thus, the new topographic  
515 information provided by the ALOS DEM does not support the existence of a megalake in this  
516 basin. This conclusion is endorsed by interpretation of the PALSAR HH imagery, which shows  
517 even more detail of the rivers, allowing the three wadis to be traced continuously from their  
518 sources to an altitude of about 200 m where they appear to have fed small lakes in localised  
519 depressions (Figure 3B).

#### 520 4.3.3 Megalake Timbuktu

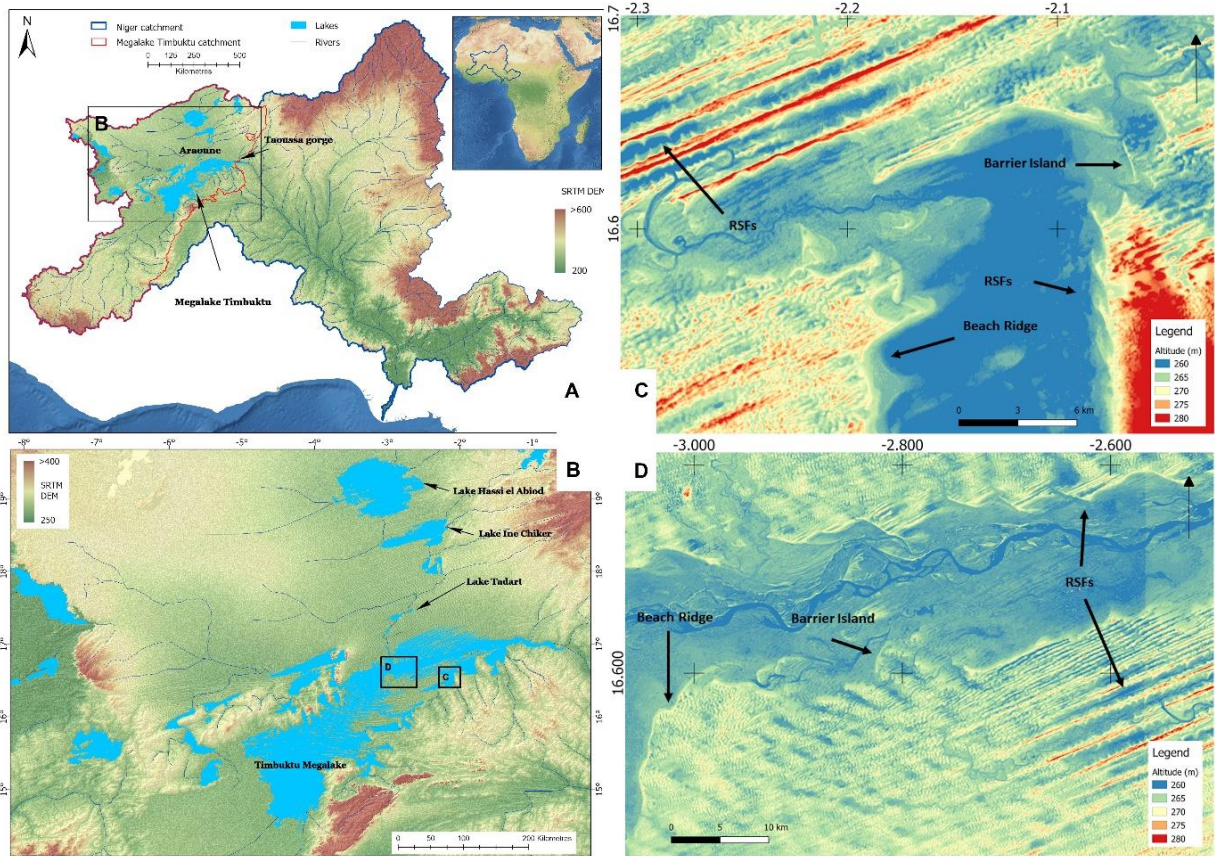
521 Using our GEE global image mosaics of the datasets discussed above, we discovered a new  
522 Saharan megalake in the vicinity of the Niger Inland Delta of Mali (Figure 6). It has long been  
523 recognised that during the last glacial maximum the delta was dry, with active dunes that  
524 blocked the Niger River valley at the Taoussa Gorge (Beaudet et al., 1977; Figure 6A). Upon  
525 the reactivation of the river during the AHP, the dunes damming the gorge are thought to  
526 have diverted a rejuvenated River Niger into the Araoune region (Beaudet et al., 1977), a  
527 large flat plain to the north of Timbuktu (Figure 6A and B). However, as the AHP progressed  
528 the River Niger cut through the dunes and its current course was established (Beaudet et al.,  
529 1977).

530 Petit-Mare and Riser (1983) investigated the Araoune region and confirmed the findings of  
531 Beaudet et al., (1977), recognising an interior delta containing a network of paleochannels

532 and abundant lake sediment outcrops. We investigated this area using satellite imagery and  
533 DEMs and find that the paleolake sediments and river channels recognised by Petit-Mare  
534 and Riser (1983) are clearly visible. However, the ALOS 30 m DEM also reveals an abundance  
535 of lake shorelines, both in the Araoune and in the Niger Inland Delta, expressed as rhythmic  
536 shoreline features (RSF), that indicate the presence of a large lake. RSF's are undulations in a  
537 shoreline that are roughly periodic in space along the shore (Walton 1999, Pruszek et al.,  
538 2008; Figure 6D). In the inland Niger Delta they are found in various shapes, sizes and  
539 wavelengths. In many cases they form sand spit like features (Figure 6D), but in other cases  
540 the protrusions of sand are at or near 90° from the shoreline (Figure 6C). They also vary  
541 significantly in size (here defined by their width) and wavelength, with the smallest RSFs  
542 discernible in the ALOS DEM exhibiting an average width of 130 m and wavelength of 288 m  
543 (Figure 6C), while the largest ones found in the Niger River valley are 6 km wide with a  
544 wavelength of 8 km (Figure 6D). RSFs are usually rare shoreline landforms, but are common  
545 in this region of Mali, being found adorning the majority of paleolakes in the region (e.g. see  
546 figure 8A and B).

547 RSFs at an altitude of 264 m are found along the northern margin of the Niger River valley  
548 whilst a shoreline at the same altitude occurs on the southern margin but in this case it is  
549 composed of beach ridges and barrier islands (Figure 6D). Thus, a large lake must have  
550 existed here in the past. Shorelines adorned largely with RSFs, but also sometimes exhibiting  
551 beach ridge complexes and barrier islands (Figure 6C and D), are found at the same altitude  
552 in the southern Araoune, in the large deep lakes basins to the west of Timbuktu and along  
553 the edges of the numerous lakes to the south of the River Niger (Figure 6C). All these lakes  
554 are connected to the main lake in the Niger River valley by channels that, when the water  
555 level was at 264 m, would have transferred water from the latter to the former, producing  
556 one large interconnected water body. DEM analysis shows that this lake has an area of  
557 27,352 km<sup>2</sup> and a maximum depth of 92 m, but was predominantly shallow, with a median  
558 depth of just 2 m. We have called this large expanse of water Megalake Timbuktu.

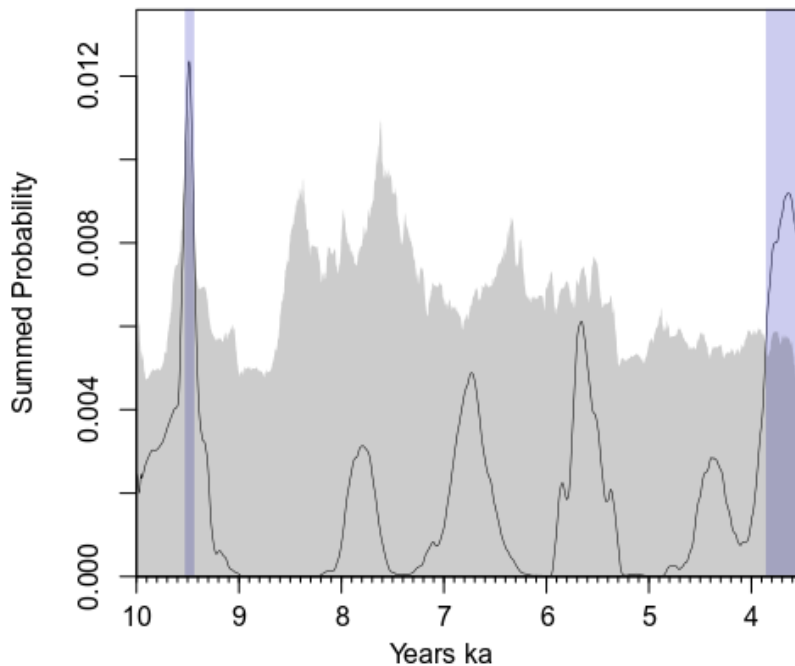




559

560 Figure 6. A) The topography of the Niger River Catchment derived from the SRTM 90 m DEM  
 561 showing the Niger River, Magalake Timbuktu, its catchment and the other large lakes within it (rivers  
 562 and lakes derived from Drake et al., 2011 apart from Megalake Timbuktu that was mapped in this  
 563 study). B) A more detailed view of the paleohydrology of Megalake Timbuktu and the Saharan  
 564 portion of its catchment. The topography is derived from the SRTM 90 m DEM and the lakes, rivers  
 565 and catchments outlined in A. C) The shoreline landforms of the Lake Aougoundoupart part of  
 566 Megalake Timbuktu as revealed by the ALOS 30 m DEM. D) ALOS 30 m DEM showing the shoreline  
 567 landforms of Megalake Timbuktu along the Niger River valley. The northern margin of the River  
 568 Niger valley is comprised of a series of large RSFs whilst smaller ones are found in the interdune  
 569 depressions to the south. Similar small RSFs can be seen in more detail in C.





570

571 Figure 7. Monte-Carlo Summed Probability Distribution plot (Shennan et al., 2013) of the 15  
 572 radiocarbon dates tested against a null hypothesis of uniform hydrological activity between 10 and  
 573 3.5 ka employing 1000 simulations. The black line shows the probability distribution for the observed  
 574 dates, the shaded grey area shows the 95% confidence interval from the simulated summed  
 575 probability distributions and the blue bars indicate areas of the probability distribution that exceed  
 576 the 95% confidence interval upper limit.

577

#### 578 4.3.3.1 The age of Megalake Timbuktu

579 Megalake Timbuktu must have developed soon after the onset of the AHP and would have  
 580 existed until the time the dune dam in Taoussa Gorge was breached. Though no direct dates  
 581 on the shorelines of Megalake Timbuktu exist, there are 15 <sup>14</sup>C dates on aquatic fossil  
 582 remains from other lakes in its catchment that shed some light on when the region was  
 583 humid, and thus provide the best data currently available for its likely age (Table 1). If we  
 584 plot the <sup>14</sup>C dates, there appears to be considerable fluctuations in the evidence for wetness  
 585 from 10 to 3.5 ka (Figure 7). However, as there are only 15 dates the plot is dominated by  
 586 the sporadic nature of the small sample size and the inevitable gaps between individual

587 calibrated dates cannot be interpreted as a decline in hydrological activity (Bleicher 2013,  
 588 Surovell et al. 2009).

589

SiteName	Latitude	Longitude	Labcode	C14 Age	C14 Error	Material	Reference
Arawan (1)	18.9000	-3.4667	UQ1021	8800	200	Mollusc	Petit-Maire and Riser 1987
Arawan (2)	19.0000	-3.5833	UQ1043	4800	100	Mollusc	Petit-Maire and Riser 1987
Azawad (1)	17.5167	-3.1000	GIF6460	3530	90	Mollusc	Petit-Maire and Riser 1987
Azawad (2)	18.0000	-3.0000	UQ1051	9250	100	Mollusc	Vernet 1998
Bou Jbeha	18.4667	-2.5667	GIF6459	3460	90	Mollusc	Petit-Maire and Riser 1987
Hassi El Abiod AR8	19.1000	-3.9167	UQ368	8450	60	Mollusc	Riser et al., 1984
Ine Chiker	18.6667	-2.5667	GIF6463	3940	90	Mollusc	Petit-Maire and Riser 1987
Jebel Tadtart	17.4167	-3.0333	GIF6461	8500	120	Mollusc	Petit-Maire and Riser 1987
Kobadi hydrology	15.3500	-5.4833	PARISVI2	3335	100	Bone	Raimbault 1986
Tin guettai AR6	19.2700	-3.5400	UQ1019	8700	200	Mollusc	Petit-Maire and Riser 1987
Tin guettai AR6	19.2700	-3.5400	UQ1078	5900	200	Mollusc	Petit-Maire and Riser 1987
Tin guettai AR6	19.2700	-3.5400	UQ370	4970	60	Mollusc	Petit-Maire and Riser 1987
Hassi el Abiod AR7	18.7300	-3.4900	GIF5495	6970	130	Bone	Petit-Maire et al., 1983.
Hassi el-Abiod	19.1167	-3.9167	GIF6462	5920	100	Mollusc	Petit-Maire et al., 1983.
Kobadi	15.3580	-5.4870	PA221	3335	100	Bone	Jousse et al., 2008.

590 Table 1. Radiocarbon dates from paleolakes within the Megalake Timbuktu catchment. Dates are  
 591 from fossil aquatic organisms found in paleolake sediments and archaeological sites on lake margins.

592

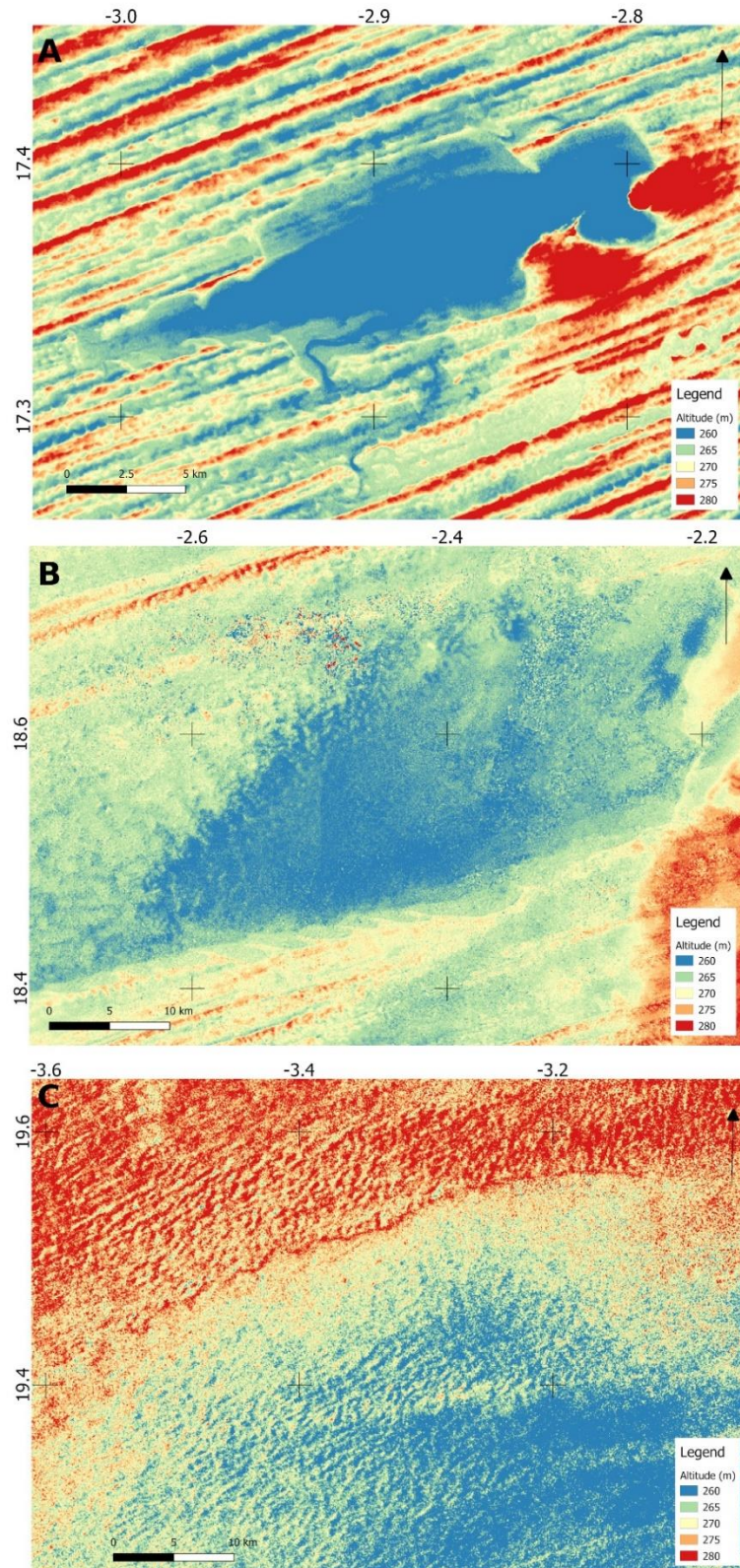
593 To test the significance of these fluctuations, we therefore use the Monte-Carlo Summed  
 594 Probability Distribution (MCSPD) method of Shennan et al., (2013), which assesses the  
 595 combined probability distribution of our 15 radiocarbon dates against a null hypothesis of  
 596 uniform hydrological activity between 10 and 3.5 ka employing 1000 simulations (Figure 7).  
 597 Our results reveal a departure from the uniform model, with two periods of increased  
 598 hydrological activity at 9.5 and 3.9-3.5 ka (p-value=0.012). Between 9.5 and 3.5 ka the  
 599 observed data does not fall outside the 95% confidence limit of the simulated data,  
 600 suggesting there is insufficient data to reject uniform hydrological activity over this period.

601 These results therefore indicate that Megalake Timbuktu became active around 9.5 ka,  
602 when we see a peak in hydrological activity and the catchment remained relatively wet until  
603 3.9 ka, at which point there was another peak in hydrological activity, which ceased at about  
604 3.3 ka. However, the demise of Megalake Timbuktu was not caused by a return to aridity,  
605 but the breaching of the dune dam in Taoussa Gorge, and this could have occurred any time  
606 between 9.5 and 3.3 ka. Given the high erodibility of dune sands and the considerable  
607 discharge of the Niger River, thus its high erosivity, the failure of the dune dam is likely to  
608 have occurred sooner rather than later and thus probably happened in the early to middle  
609 Holocene.

610

#### 611 *4.3.3.2 Erosion of shorelines in the catchment of Megalake Timbuktu*

612 There is an apparent contradiction between the excellent preservation of the Megalake  
613 Timbuktu shorelines and our argument that only fragments are preserved in deserts due to  
614 aeolian erosion and deposition. This can be explained by the fact that Megalake Timbuktu is  
615 situated on the 200 mm isohyet (Figure 1A), straddling the boundary between the Sahara  
616 and the Sahel. Here dunes were stabilised after the end of the Last Glacial, and aeolian  
617 processes are not particularly active, meaning that they retain their LGM dune form and  
618 evidence for subsequent modification by fluvial and lacustrine processes during the AHP.  
619 Moving north of the Megalake aridity increases, the dunes become more active, and the  
620 lake shorelines become less distinct as they are increasingly eroded and covered in sand. For  
621 example, 27 km north of the megalake, the shoreline of Lake Tadart (Figure 6B and Figure  
622 8A) is completely intact, clearly showing both RSFs, embayments and beach ridges. A further  
623 125 km north lies Lake Ine Chiker, with about one third of the shoreline remaining (Figure  
624 6B and Figure 8B), though it still displays well developed RSFs. Another 110 km north lies  
625 Lake Hassi el Abiod (Figure 6B and Figure 8C) where about a fifth of the shoreline is evident  
626 and this is simply a highly eroded ridge with no other diagnostic features (Figure 8C). This  
627 north-south transect supports our argument that aeolian erosion and deposition severely  
628 affect shoreline preservation in the Sahara. It clearly shows that in the sand sea of northern  
629 Mali just 262 km north of the Sahara/Sahel boundary the vast majority of the paleolake  
630 shorelines are no longer visible in remote sensing imagery or DEMs, with only fragments  
631 remaining.



632

633 Figure 8. Timbuktu catchment lakes. A) ALOS 30 m DEM of paleolake Tadart, B) paleolake Ine Chiker  
 634 and C) paleolake Hassi el Abiod. See figure 6B for their location.

635

636

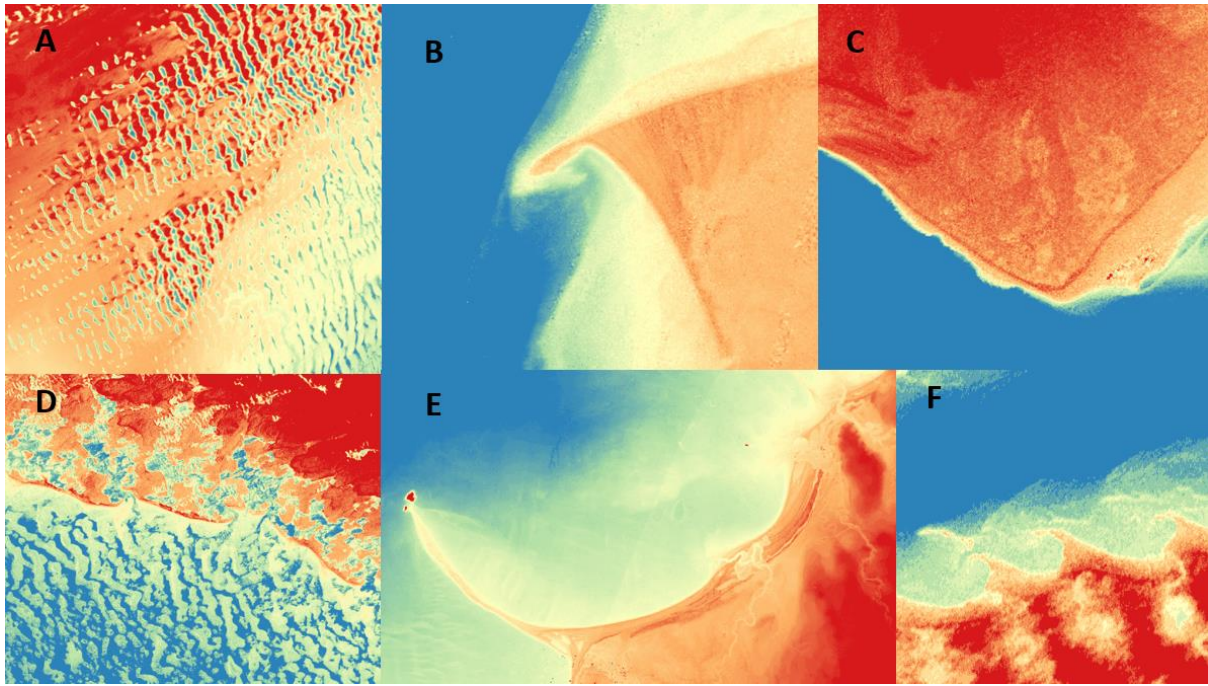
637 *4.3.4 Confidence Estimation for Remote Sensing and DEM analysis of Megalake*

638 *Geomorphology*

639 Three of the megalakes discussed above have been identified solely by interpretation of  
640 shoreline features in satellite imagery and DEMs (i.e. Darfur and Timbuktu, Tushka), and  
641 have not been verified with field evidence. Furthermore, the existence of two of these lakes  
642 has been questioned by others interpreting similar satellite imagery and DEMs (e.g.  
643 Megalake Darfur by Quade et al. (2018) and Megalake Tushka in this study). These  
644 disagreements occur because there are no formally recognised criteria using imagery and  
645 DEMs to identify palaeolakes. To overcome this problem we have developed a method that  
646 allows the interpreter to obtain different levels of confidence about the evidence for the  
647 presence of a lake in a basin during the past. We have then applied the method to all the  
648 megalakes discussed above in order to evaluate systematically the veracity of the lake  
649 shoreline evidence.

650 Our method recognises that not all shoreline landforms are equal; some are more diagnostic  
651 than others. The least diagnostic shorelines are single beach ridges or wave ravinement  
652 surfaces. This is because similar shaped landforms can be formed in other ways, thus there  
653 is an uncertainty associated with their attribution as a shoreline. Figure 9A illustrates this  
654 point, showing a break of slope overlain by sand dunes, which could be a lake ravinement  
655 shoreline or simply a reflection of variation in the topography underlying the dunes. In  
656 contrast, many coastal landforms have more diagnostic shapes, such as spits (Figure 9B),  
657 cusped headlands (Figure 9C), barrier islands (Figure 9D), beach ridge complexes (Figure  
658 9E), tombolos (Figure 9E), deltas (Figure 10A), and RSFs (Figure 9F). Thus, their identification  
659 in a closed basin provides strong evidence for the presence of a lake.





660

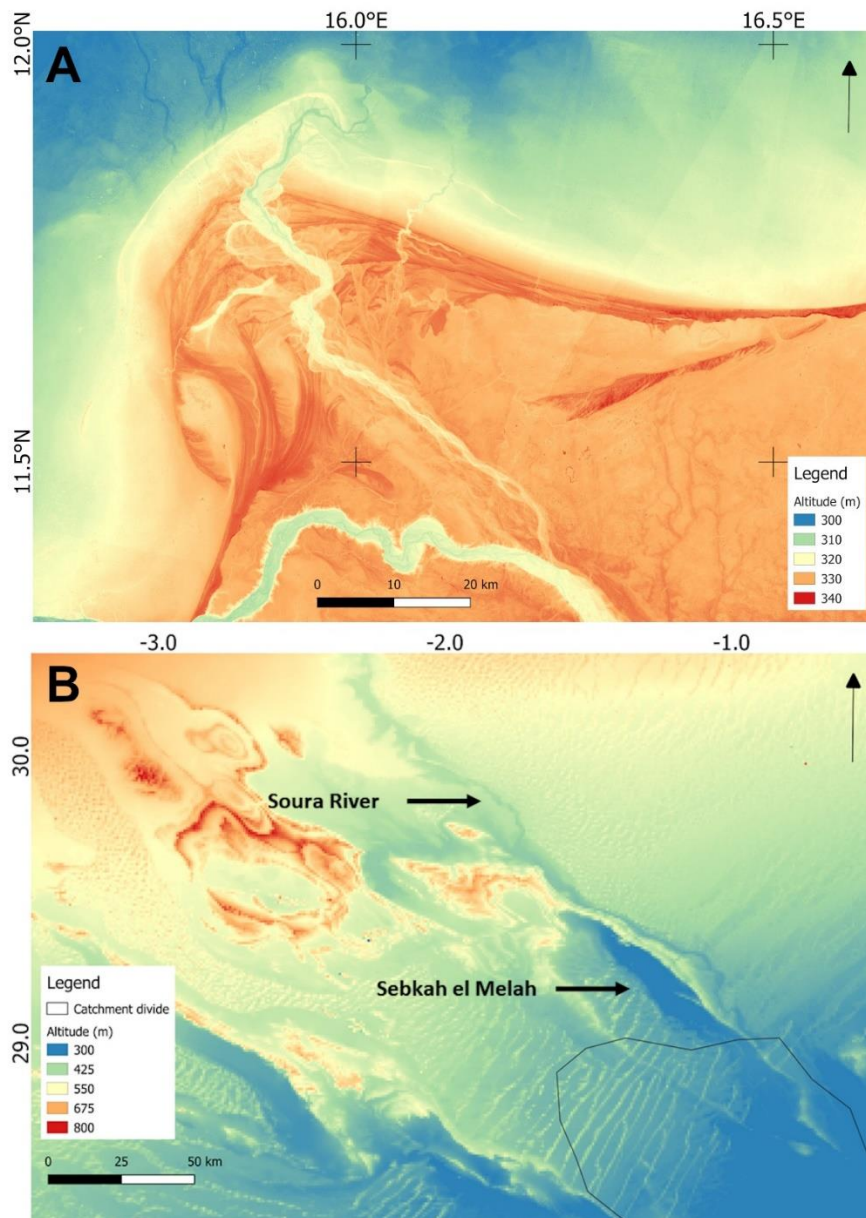
661 Figure 9. Shoreline landforms of Megalake Chad (a,b,c,d,e) and Timbuktu (f) as revealed by the ALOS  
 662 30 m DEM. A) Lake ravinement shoreline at E15.454, N13.156. B) Sand spit at E18.6446, N15.8075.  
 663 C) Angamma Delta Cuspate headland at E17.7320, N17.5631. D) Barrier islands at E13.5848,  
 664 N14.4087. E) Beach ridge complexes and Tombolo at E17.5328, N12.1363. F) RSFs at W4.3918,  
 665 N16.5749. Low elevations are displayed in blue, intermediate yellow and high red.

666

667 Unfortunately, diagnostic landforms are rare in comparison to their undiagnostic  
 668 counterparts, and are sometimes absent. In the latter case, altitudinal relationships  
 669 between the different undiagnostic shoreline landform fragments in a basin can provide  
 670 evidence for the presence of a paleolake, because all coastal landforms formed in a single  
 671 phase of lacustrine activity will be found at the same altitude. Furthermore, if the lake has  
 672 filled to the level of an outflow, the shorelines will have the same altitude as the lowest  
 673 point on the catchment rim, where a lake outflow channel may also be found.

674 Given these characteristics of shorelines it is possible to use them to assign different levels  
 675 of confidence to the identification of a paleolake in a basin. We express this confidence  
 676 using a scale of 0 (uncertain) to 5 (certain). If there is only a single small exposure of an  
 677 undiagnostic shoreline in a catchment it is not possible to demonstrate that there was a lake  
 678 in the basin (Level 0). However, extensive preservation of an undiagnostic shoreline at the  
 679 same altitude or smaller exposures at multiple locations are suggestive of the presence of a

680 lake in the basin in the past (Level 1). If these landform altitudes coincide with that of the  
 681 lowest point on the catchment rim, where lake outflow would be expected to occur, it adds  
 682 further evidence (Level 2), as does the presence of a lake outflow channel at this location  
 683 (Level 3). If a diagnostic landform is found then it is highly likely that a palaeolake existed in  
 684 the basin (Level 4), and the presence of more than one diagnostic landforms in a basin  
 685 constitutes unequivocal evidence for the presence of a palaeolake (Level 5).



686  
 687 Figure 10. A) ALOS 30m DEM of Lake Megachad's Chari Delta. The delta front is composed of  
 688 numerous different beach ridge complexes that have been incorporated into the delta as it  
 689 prograded into the megalake. B) Topography (SRTM 1 km DEM) of the Soura River region. The black  
 690 line shows the catchment boundary as mapped by Quade et al., (2018).



691

692 Applying this classification scheme to the Saharan basins where controversy exists, we find  
693 that the Darfur Megalake scores a 5 because of two diagnostic landform exposures, both at  
694 the same altitude as the lowest point on the catchment rim. Tushka Megalake scores 0  
695 because no shorelines are identified. The less controversial Megalakes Chad, White Nile and  
696 Timbuktu all score 5 due to the presence of diagnostic shoreline landforms. In contrast  
697 Megalake Fezzan, Ahnet-Mouydir and Chotts all score 0 because no shorelines have been  
698 identified by remote sensing and DEM analysis in these basins. However, the absence of  
699 shoreline features evident in images of DEMs in some basins is not unexpected given the  
700 impact of aeolian processes, though it does preclude the identification of palaeolakes using  
701 remote sensing alone. In these areas it may still be possible to identify shorelines, and  
702 therefore megalakes, on the basis of sedimentary evidence.

703

#### 704 *4.4 Sedimentary evidence for Saharan Megalakes*

705 In some of the Saharan basins it is sedimentary rather than geomorphic evidence that has  
706 been used to infer the presence of lacustrine systems. Many authors report the occurrence  
707 of shell-rich deposits and have used the altitude of these to infer the height of palaeo-lake  
708 levels. Quade et al., (2018) have suggested that many of these deposits were spring and  
709 groundwater deposits that have been mis-interpreted as lake shorelines. It is important to  
710 highlight that this suggestion is based on a study of satellite imagery and not field  
711 observations.

712 The sedimentology of the Fezzan basin has been investigated in detail. Evidence supporting  
713 the existence of Lake Megafezzan consists of outcrops of interbedded lacustrine limestones  
714 and sandstones that are protected from erosion by a layer of heavily indurated limestone.  
715 These outcrops are found throughout much the Fezzan Basin, their stratigraphy can be  
716 correlated over vast distances and dating shows that they are similar in age (Hounslow et  
717 al., (2017), thus providing conclusive evidence for a large lake. For example, the eastern  
718 margin of Lake Megafezzan is defined by a 200 km long outcrop of shallow freshwater  
719 limestone that could not have been deposited by anything but a large contiguous body of  
720 water.

721 The sedimentary evidence for the Ahnet-Mouydir megalake is comprised of numerous  
722 outcrops composed of thick sequences of lacustrine and deltaic sediments, with some  
723 sections recording the transition between these two facies indicating the progradation of  
724 the delta over the lake sediments as the water level fell. The sediments are extremely rich in  
725 organic remains, with numerous layers composed exclusively of either shells or diatoms  
726 (Conrad and Lappartient 1991). The shell layers consist primarily of *C. glaucum*, which is  
727 indicative of brackish conditions, but species such as Hydrobiidae sp. that can live in  
728 freshwater or brackish waters are also present. In some layers these species are absent and  
729 *Bithynia thomasi* and *gaudryi*, *Melanoides tuberculata* and *Planorbis* sp. dominate,  
730 suggesting a different lacustrine environment. The diatomites include 45 different species  
731 (names not reported by Conrad and Lappartient 1991) found associated with ostracods  
732 (*Potamocypris* sp., *Cyprideis cf. torosa* Jones, and *Cyprinotus cf. salinus* Brady) and  
733 foraminifera (*Ammonia beccarii* (Linnne) var. *tepida* Cushman, *Protelphidium* sp., and  
734 *Elphidium* sp.). Fish bones are also present belonging to Percidae and Siluridae families  
735 (Conrad and Lappartient 1991). The sedimentology, large spatial distribution of the lake  
736 sediment outcrops and biological diversity can only be explained by their formation by a  
737 large lake. However, at present there is a lack of information on the exact location of many  
738 of the deposits and their altitudinal relationships. Furthermore, little work has been done on  
739 the facies relationships between them. Thus there are still large gaps in our understanding  
740 of this megalake.

741 In the Chott basins much of the evidence for megalake shorelines has been described from  
742 the area around the town of Tozeur at an altitude of about 45 m (Figure 1B; Zouari et al.,  
743 1998). Tozeur is famous as an oasis resort and is surrounded by extensive date palm  
744 plantations. On studying images of the Tozeur region Quade et al., (2018) observed no  
745 shoreline features but identified at least two active springs and large patches of white  
746 sediments that they interpreted as fossil spring deposits. From this they inferred that  
747 previous authors (Causse et al., 2003; Zouari et al., 1998) had mistaken these springs for  
748 shell rich lacustrine deposits. In fact the spring features that Quade et al., (2018) identify are  
749 the termination of channels dug into the saline mudflats of the Chott el Dejrid in order to  
750 dispose of excess irrigation water from Tozeur oasis. These channels can be clearly seen in  
751 Google Earth (Figure 4B). Furthermore, fieldwork shows that the patches of white sediments

752 are the drier parts of the Chott mudflats, where efflorescent gypsum and halite crusts have  
753 started to develop on the playa surface. Nothing that Quade et al., (2018) discuss in  
754 reference to their interpretation of satellite imagery of the Chott basin relates to the  
755 features we have seen in the field, or those used to identify shorelines by Zouari et al.,  
756 (1998).

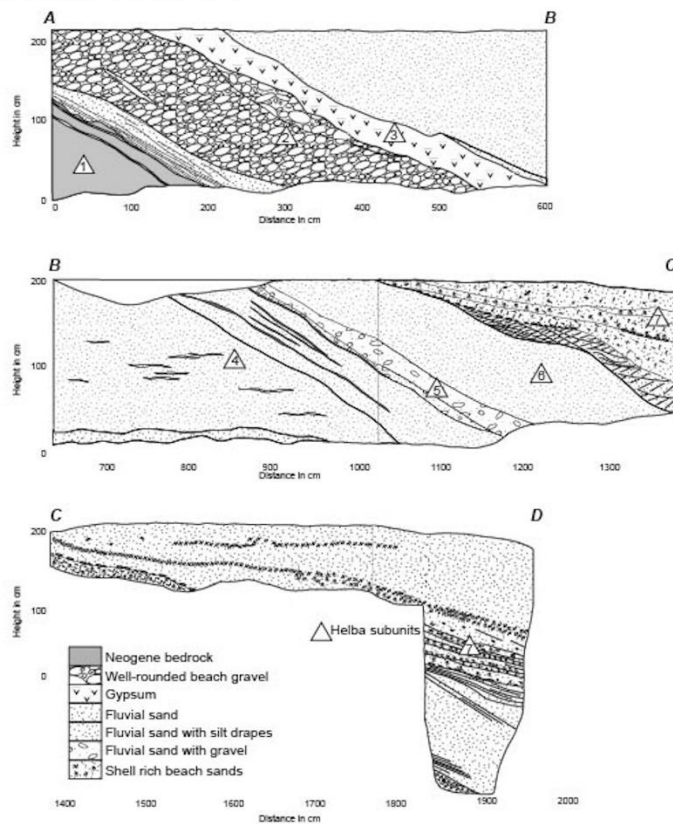
757 The shell rich deposits described by Zouari et al., (1998) are found within Tozeur oasis and  
758 are not visible on satellite imagery because of the extensive palm tree canopy. Quartz-rich  
759 sand and shell deposits are found in the Touzer region (Figure 11), stretching westwards to  
760 the town of Nefta, whilst small outcrops of similar deposits have been reported in the Chott  
761 el Djerid basin across a distance of 150 km (Figure 1B; Coque 1962). Whilst Quade et al.,  
762 (2018) have argued that these sediments should be interpreted as spring deposits, they are  
763 overwhelmingly dominated by a single species, the bivalve *C. glaucum* (Richards and Vita-  
764 Finzi, 1982; Causse et al., 1989; Zouari et al., 1998) indicating brackish conditions (Figure 11  
765 (right) A). Modern springs in the Tozeur region contain no *C. glaucum* because they produce  
766 potable water, and are instead dominated by *Melanoides tuberculata*, implying that the two  
767 species are indicative of different depositional environments (Roberts and Mitchell, 1987).  
768 The *C. glaucum* shells within the proposed shoreline deposits are rarely in life position or  
769 articulated. Instead, they show evidence for current transport and occur within sandy  
770 deposits characterised by well-rounded pebble clasts (Figure 11 (right) B) and well-  
771 developed cross-bedding (Figure 11 (right) C and D). Disarticulated shells in cross-bedded  
772 sands and gravels are typical of shells that have been hydrodynamically sorted by traction  
773 currents and are common in beach shoreface environments (Reineck and Singh, 1980).  
774 Conversely, springs in the region typically produce spring mounds which are formed when  
775 gypsiferous aeolian dune sands are trapped by vegetation growing around the spring. These  
776 mounds typically display a complex stratigraphy with organic layers, root casts/traces and  
777 wash deposits dipping away from the water source and a molluscan fauna that is dominated  
778 by *Melanoides tuberculata* (Roberts and Mitchell, 1987). A final notable difference between  
779 springs and beach deposits is their altitude. Beach deposits are found clustered around 45 m  
780 because, in this basin this is the maximum altitude that lake waters could reach before  
781 overtopping a col that allows outflow into the Mediterranean Sea (Figure 1A). In contrast,  
782 spring deposits are found at a wide variety of altitudes, reflecting local variations in the

783 position of the water table and the nature of the underlying rock strata. Consequently,  
 784 spring and beach deposits are readily differentiated in the field, and we concur with Zouari  
 785 et al., (1998) in their identification of shell rich shorelines in the Chott el Djerid region of  
 786 Tunisia.

**Helba section outline**



**Helba sections detail**



787

788 Figure 11. The figure on the right shows the sedimentary section of the lake shoreline outcrop at  
 789 Helba Oasis. The full section is outlined at the top but has been split into three to allow the full detail  
 790 to be presented. The seven subunits that make up the sequence consist of; 1) Neogene bedrock, 2)  
 791 well-rounded clast rich deposits (shoreface), 3) gypsum (desiccating lake basin), 4,5,6) red fine-  
 792 grained terrigenous sands (fluvial/sheetwash during low stand), 7) cross-bedded sands rich in  
 793 unarticulated *C. glaucum* (shoreface). The photos on the left show the Characteristic sedimentary  
 794 features of the palaeo-shoreline deposits in the locality of Tozeur. A) Comminuted shell beds  
 795 showing disarticulated valves of *C. glaucum*. Such beds are typical of shells transported and

796 deposited by strong current flow processes. B) Palaeo-shoreline surface showing *C. glaucum* shells  
797 and well-rounded quartz clasts, the latter being the typical product of tractional shoreline currents.  
798 C) and D) cross-bedding within the palaeo-shoreline deposits at a range of scales, representing small-  
799 scale bedforms (C) and shoreface deposition (D).

800

801 The nature of shoreline deposits in this region can be illustrated using the site of Helba,  
802 located near the town of Tozeur. The deposit consists of medium/coarse sands with  
803 occasional fine pebbles and accumulations of disarticulated and reworked *C. glaucum* shells.  
804 The sands are typically cross-bedded. This sequence is shown in Figure 11 (left) and consists  
805 of 7 main stratigraphic units (listed from the base up): Subunit 1 consists of Neogene  
806 bedrock composed of gypsum and clays, subunit 2 is a deposit consisting of rounded gravel  
807 clasts and sand lenses, subunit 3 is a gypsum unit, subunits 4, 5, 6 are reddened fine sands  
808 and silts with clay drapes reflecting deposition of terrigenous deposits by fluvial processes  
809 and surface wash, subunit 7 consist of quartz-rich sands with beds of *C. glaucum* shells. This  
810 sequence is interpreted as containing two discrete shoreline deposits (subunits 2 and 7),  
811 coincident with high lake levels, separated by low stand deposits (subunits 3-6). These low  
812 stand deposits consist of an initial unit of gypsum accumulation (evaporite concentration  
813 and precipitation during lake desiccation, subunit 3) followed by the erosion and deposition  
814 of sediments by sheetwash and fluvial activity (subunits 4-6) during a period of low lake  
815 level.

816 The facies relationships between the high and low-stand deposits reflect lake rather than  
817 spring deposits. Furthermore, neither of the two shoreline deposits (subunit 2 and 7) can be  
818 interpreted as spring-line or groundwater deposits. Subunit 2 meets the criteria of a  
819 shoreline deposit as laid out by Quade et al. (2018), since it consists of well-rounded clasts.  
820 These sediments are typical of the accumulation of clastic material that has been rolled by  
821 wave processes along a littoral, shoreline environment. Whilst subunit 7 is not clast rich, the  
822 cross-bedding within the sands and the well-sorted nature of the sediments indicates that  
823 they are the result of current flow processes, whilst the abundance of *C. glaucum* shells  
824 supports the idea that this was current flow in association with brackish water. The  
825 deposition of sand by coastal processes associated with a large brackish water body can only  
826 be explained by shoreline processes operating in association with a lake system. As the

827 formation of a lake shoreline at the altitude of Helba (40m) requires most of the Chotts to  
828 be flooded, the occurrence of these sediments requires the existence of a megalake.

829 The Helba sequences highlights the disadvantages inherent in trying to identify lake  
830 shorelines in the Sahara using remote sensing alone, since the shoreline deposit is buried by  
831 younger terrigenous sediments, obscuring it from view. This phenomenon is common in the  
832 Chott basin, and deposits rich in *C. glaucum* shells are often overlain by several meters of  
833 terrigenous sediments. Combined with the preferential location of oasis agriculture on  
834 these deposits, owing to their good drainage and low salinity, this makes the identification  
835 of continuous shorelines in the Chott basin via remote sensing problematic. In conclusion,  
836 the Chott el Djerid basin contains well-preserved shoreline sedimentary sections that  
837 contain clear evidence for an extensive lake system. The absence of shoreline landforms can  
838 be explained by erosion, burial or human activity.

839 From the above review of megalake sedimentology it can be concluded that in order for  
840 there to be strong sedimentary evidence for a megalake, the deposits must satisfy two  
841 criteria. Firstly, they must show evidence that the sediments are lacustrine not palustrine;  
842 all the megalakes discussed above meet this criterion. Secondly, they must exhibit  
843 sedimentary characteristics that can only be formed by a large lake. Here the strength of  
844 evidence varies. For Megalake Fezzan the evidence is strong with lacustrine sediments  
845 distributed over large areas. Evidence is also strong for the Chotts Megalake, with a  
846 multitude of shoreline sediment exposures exhibiting similar sedimentology found at a  
847 similar altitude around the basin. For the Ahnet-Mouydir Megalake the evidence is less  
848 strong. Although there are a number of lake sediment outcrops, their exact location and the  
849 altitudinal and facies relationships between them are as yet unclear.

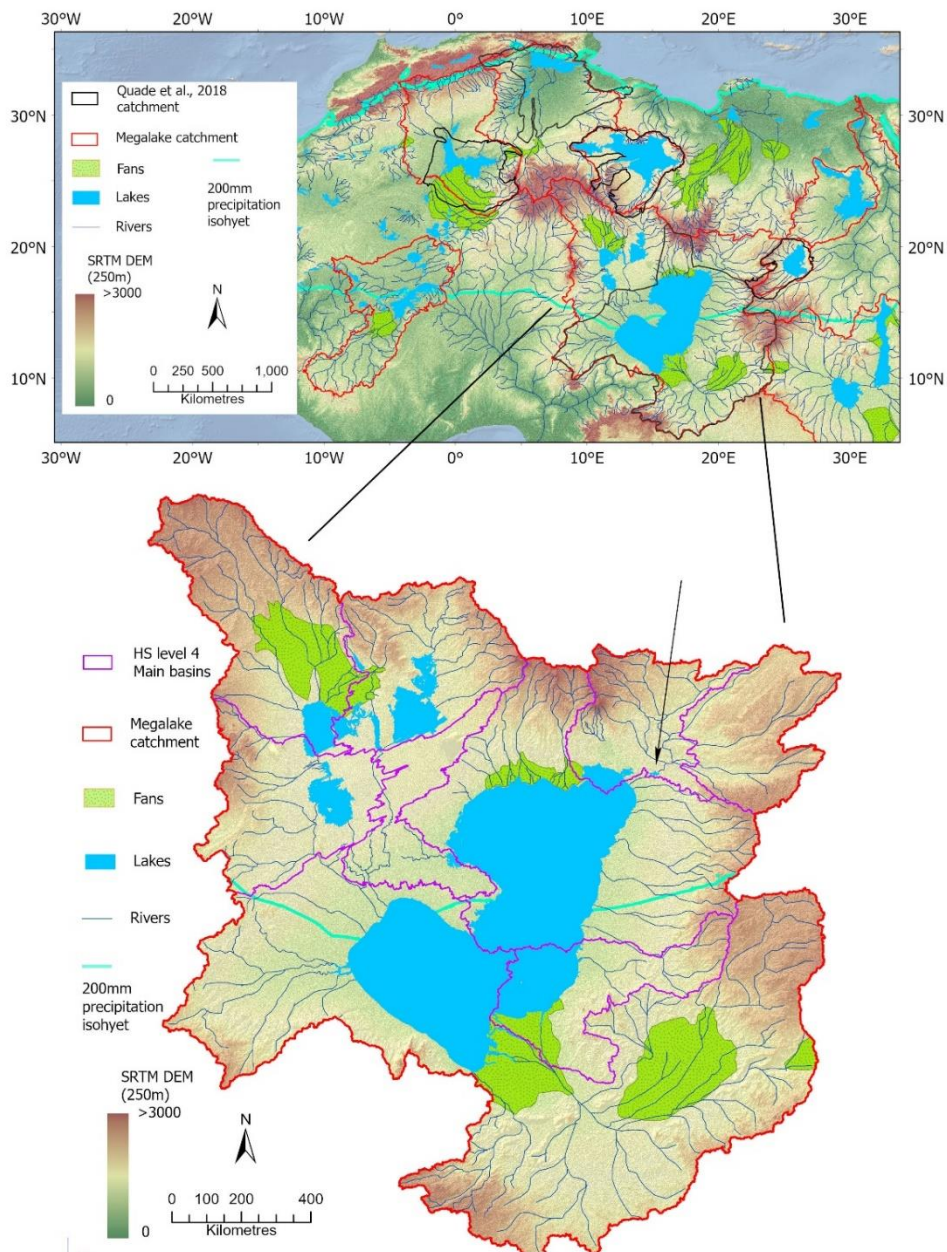
850

## 851 **5. Catchment Mapping and Rainfall Estimation**

852 Quade et al., (2018) use the catchment size and past/present rainfall regimes of the Saharan  
853 megalakes in a modelling exercise, concluding that it was not feasible for megalakes to have  
854 existed during the Holocene AHP. However, in most cases the catchment areas used by  
855 Quade et al., (2018) were significantly smaller than those used in this paper (Drake et al.,  
856 2011; Figure 12 (top) and Table 2) and previously published estimates (e.g. Servant and



857 Servant, 1983; Schuster et al., 2005 for Lake Megachad). As a result, Quade et al., (2018)  
 858 exclude a number of major tributary systems from their analysis that would have been  
 859 important sources of runoff for Saharan megalakes. Furthermore, in most cases the  
 860 catchments proposed by Quade et al. (2018) do not include mountains which form one of  
 861 the main moisture sources for several Saharan megalakes, particularly in their function as  
 862 ‘water towers’ (Lezine et al., 2011; Figure 12 (top)).



863

864 Figure 12. Top: Map showing the topography (SRTM 1 km DEM) and paleohydrology of North Africa  
 865 with a comparison of the Quade et al. (2018) and Drake et al. (2011) megalake catchments. Bottom:  
 866 Megalake Chad catchment topography (SRTM 90 m DEM) showing the lakes mapped by Drake et al.,



867 (2011) and their sub-catchments as defined by the HydroSHEDS level 4 catchments. The arrow  
868 highlights a small lake not readily evident to the eye.

869

870 In our analysis the megalake catchments of Drake et al., (2011) were used. These were  
871 produced by manual digitisation from the SRTM 1 km DEM. Firstly, the rivers that fed the  
872 megalake were digitised from their mouth to source, including the main tributary channels  
873 encountered along the way. The catchment boundary, located at the source of these  
874 channels, was then digitised by tracing along the catchment divide defined by the channel  
875 headwaters. Furthermore, it was assumed that when the megalake existed, the entire  
876 catchment would be humid in order to sustain such large volumes of water in the lake.  
877 Under these conditions the sub-basins within the megalake catchment would contain  
878 paleolakes and it would be wet enough for these lakes to fill to overflow and feed their  
879 excess waters into the megalake in question, just as lakes do in more temperate regions  
880 today. Thus, all lake sub-basins were included within the megalake catchments. This is  
881 illustrated well by the Megalake Chad catchment that contains many substantial lakes in the  
882 north, which form in numerous different sub-catchments (Figure 12 bottom).

883 Quade et al., (2018) provide insufficient detail to precisely replicate their catchment area  
884 estimates. However, in many cases their catchments terminate where there are paleolake  
885 sub-catchments. This suggests standard GIS catchment mapping techniques (e.g. ArcGIS)  
886 have been used to define catchments, as they treat each lake basin as a separate  
887 catchment. For example, Quade et al., (2018) exclude all the sub-catchments of Megalake  
888 Chad that contain lakes (Figure 12 top and bottom). However, perhaps the best example of  
889 the problems caused by this approach occurs when defining the catchment of Megalake  
890 Ahnet-Mouydir. The northernmost margin of this catchment is defined by the headwaters of  
891 the Soura River (Conrad, 1970), the largest of a number of rivers that flow from the Atlas  
892 Mountains, feeding moisture into the Sahara (Figures 1A and 12 (top)). Quade et al., (2018)  
893 exclude much of this river from their catchment, instead placing the boundary 460 km south  
894 of the Soura River headwaters, at the point where the river feeds into Sebkah el Melah, a  
895 small lake that exists along the river's course (Figure 10B). Since the ALOS 30 m DEM clearly  
896 shows the Soura River flowing into and out of the lake and onwards into the Sahara, there is  
897 no justification for terminating the megalake catchment boundary here. Thus, it would

898 appear that standard GIS based catchment mapping methods have been employed by  
 899 Quade et al (2018) and this has resulted in sub-catchments being defined as separate  
 900 entities, such as that of the Sebkah el Melah and the lakes in the north of the Megalake  
 901 Chad catchment.

<b>Megalake Catchment</b>	<b>Drake et al (km<sup>2</sup>)</b>	<b>Quade et al (km<sup>2</sup>)</b>
White Nile	2,188,386	n/a
Chad	2,458,720	1,611,234
Timbuktu	736,989	n/a
Darfur	126,556	142,394
Tushka	316,256	n/a
Fezzan	378,429	330,221
Chotts	829,370	377,765
Ahnet-Mouydir	740,447	329,180
Total	7,775,153	2,790,794

902

903 Table 2. Catchment areas of Saharan megalakes as estimated by Quade et al., (2018) and in this  
 904 paper.

905

906 As noted above, Drake et al., (2011) assumed that the entire catchment is humid in order to  
 907 be able to sustain a megalake, and that all lake sub-basins are full to overflow. In contrast  
 908 the catchments of Quade et al., (2018) are much smaller because they terminate as soon as  
 909 they reach a lake sub-basin. Thus in terms of catchment size, the two approaches are  
 910 endmembers in a continuum, one representing wet conditions, the other dry. It is possible  
 911 that a megalake could be sustained somewhere between these extremes, with lakes in small  
 912 parts of the catchment not overflowing into the megalake. However, the method of Quade  
 913 et al., (2018) implicitly assumes a relatively dry climate in all sub-catchments, with  
 914 insufficient rainfall to allow any of them to fill to overflow. It is very unlikely that a megalake  
 915 could be sustained under these conditions and this assumption has resulted in  
 916 underestimation of the extent of most of the megalake catchments (Table 2).

917 In some cases there is clear evidence for sub-catchment lakes filling and outflowing into a  
918 megalake basin. For example, the role of the Soura River as a significant water source to  
919 megalake Ahnet-Mouydir is well known, having been discussed in detail by Conrad (1970).  
920 Furthermore, Dumont (1987) reports that the Soura was perennial as far south as Reggane  
921 in the centre of the Ahnet-Mouydir basin during historical times, and that it was still  
922 periodically active recently, reportedly flowing 800 km into the Sahara at least once during  
923 the 20th century (Dumont 1987). Investigation of MODIS satellite imagery of the river shows  
924 that as recently as 2014, severe flooding in the Atlas Mountains activated the river and  
925 brought floodwater 550 km into the desert, filling Sebkah el Melah and then flowing  
926 onwards towards Reganne. Importantly, the Soura River is only one of three large rivers  
927 draining the Atlas Mountains that would have fed megalake Ahnet-Mouydir during past  
928 humid periods (Figure 1A; Drake et al., 2011), with the lake thus receiving a considerable  
929 amount of runoff from this region. However, none of these rivers are included in the Ahnet-  
930 Mouydir catchment of Quade et al., (2018), producing a severe underestimation of the  
931 moisture received by this megalake.

932 An important problem with such underestimations of catchment area is that they tend to  
933 exclude mountainous regions, those parts of the catchment with the highest rainfall, and  
934 which play an important role in regional hydrological responses during humid episodes  
935 (Lezine et al., 2011). In the example above, by excluding the Atlas Mountains from the  
936 reconstruction of the Ahnet-Mouydir catchment, an area of significantly higher annual  
937 rainfall from outside the Sahara is excluded from the modelling of the lake budget.  
938 However, even in cases where the catchment mapping of Quade et al., (2018) matches that  
939 of previous studies, the authors tend to underestimate rainfall. Quade et al., (2018) state  
940 that, with the exception of megalake Chad, the other proposed Saharan megalakes occur  
941 “where the contributing watersheds are confined between 15°N and 35°N in areas that  
942 receive <<100mm/yr (rainfall) today”. Yet according to the WorldClim global annual average  
943 rainfall maps (Fick and Hijmans, 2017), the headwaters of the Soura River in the Ahnet-  
944 Mouydir basin receives 356 mm/a rainfall, whilst one of the rivers draining into the Chotts  
945 receives 700 mm/a (Fick and Hijmans, 2017), much higher than the <<100 mm/yr proposed  
946 by Quade et al., (2018). Furthermore, during humid periods rainfall in the Atlas Mountains

947 was much higher than at present (Zielhofer et al., 2017), exacerbating the underestimation  
948 caused by any exclusion of contributions from the Atlas Mountains.

949 In summary, the catchment mapping of Quade et al., (2018) underestimates the size of  
950 many of the proposed megalake catchments, and consequently underestimates the  
951 precipitation falling within them. In addition, Quade et al., (2018) justify their modelling  
952 results by comparing them to global paleoclimate modelling studies which are known to fail  
953 to produce a green Sahara during the AHP (Claussen et al., 2017), despite a well-  
954 documented tendency for such models to underestimate rainfall in the region at this time  
955 (Hopcroft et al., 2017). Consequently, we question the accuracy and completeness of the  
956 mass balance hydrologic modelling presented in Quade et al., (2018) and resultant  
957 assertions that the megalakes in question are hydrologically implausible.

958

## 959 **6. Chronological evidence for the timing of megalake development**

960 The evidence presented above shows that there is robust evidence for the existence of  
961 Quaternary megalakes in the Nile, Niger, Chad, Chott, Ahnet-Mouydir and Darfur basins.  
962 However, it is clear from the literature that the timing of the development of many of these  
963 megalakes is poorly constrained. There are two reasons for this. Firstly, many megalake  
964 sediments frequently contain little dateable material. Organic material suitable for  $^{14}\text{C}$   
965 dating is poorly preserved in arid regions and often researchers have relied on dating fossil  
966 shells. Both  $^{14}\text{C}$  or U/Th disequilibria techniques yield notoriously unreliable ages for fossil  
967 shells due to reservoir effects, dead carbon, diagenesis and the porous nature of freshwater  
968 mollusc shells (Walker, 2005). Whilst luminescence techniques have the potential to reliably  
969 date the quartz-rich sand shorelines found in many of these basins, this technique has only  
970 been applied to the White Nile, Chad and Fezzan basins (Williams et al., 2003; Barrows et  
971 al., 2014; Armitage et al., 2007, Armitage et al., 2015; Drake et al., 2011; Drake et al., 2018).

972 For Megalake Timbuktu there are currently no direct dates. However, our analysis of dates  
973 from other paleolakes in its catchment suggest that it developed at about 9.5 ka and its  
974 geomorphology indicates it had reached its demise by the middle Holocene. In the Darfur  
975 basin no dates are available for the high stand shoreline, though the smaller AHP lake is well  
976 dated (Hoelzmann et al., 2000; 2001). In the Ahnet-Mouydir and Chotts Megalake basins,

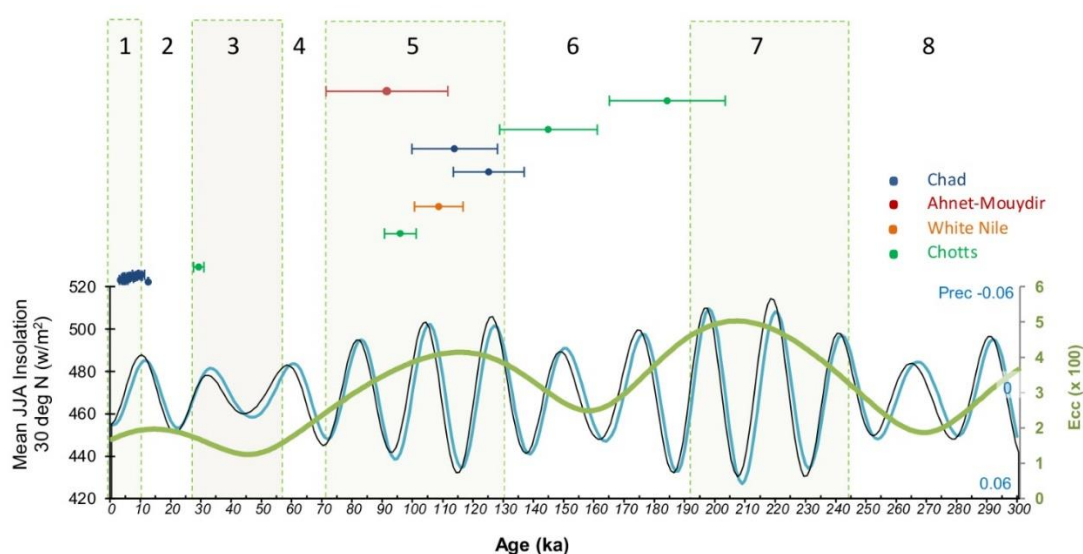
977 the only chronological information for the lake is U/Th dating of shells, a notoriously  
978 unreliable method. Thus, of the megalakes where dating has been attempted, the Ahnet-  
979 Mouydir and Chotts Megalakes are the least securely dated. Despite these limitations, the  
980 dating evidence that is available can be used to make some observations about the timing of  
981 megalake formation in the Sahara. Firstly, megalake Chad and Timbuktu provide a very large  
982 area of surface water in the southern Sahara and Sahel during the AHP. However, only in the  
983 Chad basin does a reliable chronology for a Holocene megalake exist (Armitage et al., 2015).  
984 Combined luminescence and  $^{14}\text{C}$  dating shows that the main megalake phase occurred from  
985  $\sim 11$  to  $\sim 5$  ka (Armitage et al., 2015). Pre-Holocene shorelines are much rarer in the Chad  
986 basin and only two have currently been dated, providing luminescence ages of  $114.2 \pm 14$   
987 and  $125.4 \pm 11.6$  ka (Drake et al., 2011).

988 In none of the other basins does the existing chronology indicate the establishment of  
989 megalakes during the AHP, though substantial lakes are found within them at this time;  
990 White Nile ( $4690 \text{ km}^2$ ), Darfur ( $5330 \text{ km}^2$ ) and Fezzan ( $210 \text{ km}^2$ ). The White Nile Megalake  
991 shoreline has been dated using  $^{10}\text{Be}$  to  $109 \pm 8$  ka (Barrows et al., 2014). In contrast the  
992 Fezzan megalake development is a phenomenon of the Miocene (Hounslow et al., 2018).  
993 Whilst there is clear evidence for lake formation during humid phases associated with MIS 5  
994 (Armitage et al., 2007; Drake et al., 2018) and the early-mid Holocene (Drake et al., 2018),  
995 these are much smaller water bodies with a maximum surface area of  $\sim 1600 \text{ km}^2$  (Drake et  
996 al 2018).

997 In the Chott basin, Richards and Vita-Finzi (1982) presented  $^{14}\text{C}$  ages for *C. glaucum* shells  
998 between 35 and 25 ka, close to the age limit of radiocarbon techniques at that time. Causse  
999 et al., (2003) used U/Th disequilibrium techniques to date shells from similar deposits and  
1000 identified high stands at  $30.2 \pm 1.7$ ,  $96.4 \pm 5.2$ ,  $145 \pm 16$  and  $184 \pm 19$  ka. Currently no dating  
1001 evidence exists to indicate that a megalake developed in the Chott basins during the AHP. A  
1002 similar pattern is seen in the Ahnet-Mouydir basin where U/Th disequilibrium work on shells  
1003 from nearshore sediments yields an age estimate of  $92 + 20 - 18$  ka (Causse et al., 1988).  
1004 Though luminescence dating of these deposits is required to generate a more secure  
1005 chronology, the U/Th ages do imply megalake formation during MIS 5 rather than the AHP.

1006 In summary, apart from at the southern margin of the Sahara (the Chad basin and Niger  
1007 Inland Delta) there is negligible evidence for megalake development during the AHP. Whilst

1008 all basins apart from Tushka, contain reliable evidence for megalake formation, these lakes  
 1009 mostly formed during earlier interglacial or “warm” marine isotopic stages, and  
 1010 predominantly date to MIS 5. Furthermore, for those basins that exhibit both AHP and  
 1011 earlier lake records, the AHP lakes are always considerably smaller. This implies that across  
 1012 most of Saharan Africa, the AHP was significantly drier than MIS 5. However, even in a  
 1013 period like MIS 5 there is no consistent pattern of megalake development. Whilst the Chad,  
 1014 White Nile, Ahnet-Mouydir and the Chott basins experienced megalake development, lakes  
 1015 in the Fezzan basin during this time interval are relatively localised.



1016  
 1017 Figure 13. Dates of Saharan Megalakes compared to precession, eccentricity and total insolation for  
 1018 the central Sahara (30 degree north) from to present 250 ka.

1019  
 1020 In the literature it has been widely proposed that humid phases in the northern hemisphere  
 1021 low latitudes correspond to peaks in insolation, when the inter-tropical convergence zone  
 1022 (ITCZ) is situated further north and the monsoon increases in strength (deMenocal et al.,  
 1023 2000; Prell and Kutzbach 1987). The limited and relatively imprecise dating of mega-lake  
 1024 shorelines discussed above, means that definitively correlating relic shoreline features with  
 1025 specific insolation peaks is problematic (Figure 13). For example, whilst it is clear that MIS 5  
 1026 is a period when megalake formation is recorded in a number of Saharan basins, rarely are  
 1027 the uncertainties associated with the age estimates derived from shoreline sediments  
 1028 precise enough to allow a robust correlation to individual insolation peaks or substages

1029 within MIS 5. Nonetheless, there is nothing in the dataset presented here that refutes the  
1030 idea that insolation peaks drive the occurrence of humid phases. There is extensive  
1031 evidence for the formation of megalakes during MIS5, and this period is characterised by  
1032 three pronounced insolation peaks (Figure 13).

1033

1034 If insolation peaks are the driver of mega-lake development in the Sahara, it is noticeable  
1035 that the insolation peak associated with the Holocene (Figure 13) is less intense than all of  
1036 the peaks associated with MIS 5 (5e, 5c, 5a) and MIS 7 (7e, 7c, 7a), and is only marginally  
1037 stronger than that associated with MIS 3 (Prell and Kutzbach 1987). Consequently, the  
1038 apparent dryness of the AHP relative to previous humid periods is explainable by  
1039 contemporary orbital parameters. If it is assumed that the intensity of the insolation  
1040 maximum controls the degree to which the ITCZ shifts northwards, then it is unsurprising  
1041 that the AHP was drier than previous humid periods, particularly in the northern basins of  
1042 the region most distal from the starting point for a monsoon incursion (i.e. the Chott and  
1043 Ahnet-Mouydir basins). In this context it is unremarkable that Quade et al., (2018) argue  
1044 that the AHP was not wet enough to generate megalakes. With the exception of megalake  
1045 Chad and Timbuktu, which both source water from outside the desert, our review highlights  
1046 that no researchers currently propose the existence of AHP megalakes in the Sahara.

1047

## 1048 **7. Summary and Conclusions**

1049 Geomorphic and sedimentary evidence for the formation of megalakes can be found in the  
1050 Chad, Niger, Chotts, Fezzan, Ahnet-Mouydir, White Nile and Darfur basins of the Sahara.  
1051 However, no single criterion can be used as a means of identifying a former megalake. This  
1052 is primarily because the aeolian systems of the Sahara are so dynamic that landform and  
1053 sedimentary evidence for megalakes can be easily removed or obscured, resulting in a  
1054 sparsely preserved record. Sweezy (2003) estimated that because erosion predominates in  
1055 this landscape, none of the palaeolake deposits of the Chott megalake would ultimately be  
1056 preserved in the geological record. Consequently, a strict criterion requiring well-defined  
1057 and spatially extensive shorelines for the reliable identification of a megalake is not usefully  
1058 applicable in the Sahara. Rather, a holistic approach must be taken. This must consider  
1059 geomorphic, sedimentary and fossil evidence, and evaluate the environmental significance



1060 of that evidence, rather than relying solely on the identification of extensive shorelines  
1061 using remote sensing. Although imagery and DEM analysis alone has been used to identify  
1062 some Saharan palaeolakes, the use of different criteria has produced contradictory results.  
1063 To overcome this problem we have developed a method to evaluate systematically all the  
1064 shoreline evidence in a basin. This method yields a categorical assessment of the strength of  
1065 evidence supporting recognition of a paleolake. Applying this method to the Sahara  
1066 demonstrates that strong evidence exists for two of the megalakes that have been  
1067 identified using remote sensing and DEM analysis alone (Darfur and Timbuktu), but not for  
1068 the third (Tushka).

1069 Our production of linked global mosaics of key remote sensing datasets in GEE has allowed  
1070 rapid interpretation of a wide variety of satellite imagery and DEMs. This proved to be very  
1071 effective, allowing intercomparison of the utility of these different types of remote sensing  
1072 imagery and DEMs for shoreline identification and mapping. Our analyses found the ALOS  
1073 30 m DEM to be the most useful data source, but both radar and visible and infrared  
1074 imagery provided important ancillary detail in many cases. These data allowed the  
1075 recognition of a megalake in the Niger Inland Delta region of Mali for the first time, that we  
1076 christened Megalake Timbuktu. Furthermore, interpretation of this imagery provided new  
1077 evidence to support the existence of some of the previously postulated megalakes.

1078 The understanding of the hydrology of humid phases, and the robust modelling of lake mass  
1079 balance, requires an accurate reconstruction of lake catchments. The presence of megalakes  
1080 in the Sahara was questioned by Quade et al., (2018) on the basis of a mass balance model  
1081 and a perceived absence of shoreline features. Critically, our analyses contradict this  
1082 interpretation, demonstrating that shorelines are not a diagnostic criteria for lake presence  
1083 in the Sahara due to the geomorphological dynamics of the region, and that key parts of the  
1084 fluvial networks that feed Saharan megalake basins were omitted from the mass balance  
1085 calculation, leading to substantial underestimates the runoff available to these systems. This  
1086 is particularly true in the case of the Ahnet-Mouydir basins, where the Atlas Mountains, the  
1087 wettest part of the catchment in the present day, was omitted by Quade et al., (2018).

1088 Finally this review draws two key conclusions which are in concord with the work of Quade  
1089 et al., (2018):

- 1090 1) The chronology of Saharan megalake deposits is currently poor. Consequently, the  
1091 climatic history that these deposits and landforms hold is under-developed and  
1092 efforts should be made to rectify this. With an improved chronology of these regions  
1093 it will be possible to produce robust histories for megalake development in individual  
1094 basins and, consequently, understand regional synchronicity/asynchronicity in the  
1095 timing of megalake highstands.
- 1096 2) Megalake formation is not a feature of the AHP, with the exception of megalakes  
1097 Timbuktu and Chad. As a consequence, the Holocene of the Sahara would appear  
1098 less ‘wet’ than Pleistocene humid phases such as those in MIS 5. Although the AHP  
1099 was characterised by a humid and green Sahara, the landscape and geomorphic  
1100 systems operating within this region during the Holocene were very different from  
1101 those of Pleistocene interglacials. This has implications for human dispersal across,  
1102 and occupation within, this region during the Holocene relative to MIS 5. It is likely  
1103 that the “drier” conditions which prevailed during the AHP relative to earlier humid  
1104 periods are a consequence of the relatively weak summer insolation peak which  
1105 occurs during the Holocene.

## 1106 **Acknowledgements**

1107 We would like to thank National Geographic (grant number GEFNE154-15) for funding the  
1108 Tunisian fieldwork. SJA’s contribution to this work was partly supported by the Research  
1109 Council of Norway, through its Centres of Excellence funding scheme, SFF Centre for Early  
1110 Sapiens Behaviour (SapienCE), project number 262618. Work by ND, KM & PSB was  
1111 supported by the Leverhulme Trust (grants RPG-2016-115 & ECF-2019-538). J-LS and DP  
1112 acknowledge support from the University of Oxford and from UKRI-NERC under  
1113 NE/T001313/1.

1114

## 1115 **References**

1116 Armitage, S. J., Bristow, C. S., Drake, N. A. 2015. West African monsoon dynamics inferred  
1117 from abrupt fluctuations of Lake Mega-Chad. *Proc. Natl. Acad. Sci. U S A* 112, 8543-  
1118 8548.

- 1119 Armitage, S.J., Drake, N.A., Stokes, S., El-Hawat, A., Salem, M.J., White, K. Turner, P.  
 1120 McLaren, S. J. (2007) Multiple phases of North African humidity recorded in  
 1121 lacustrine sediments from the Fazzan Basin, Libyan Sahara. *Quat. Geochronol.* 2, 181-  
 1122 186.
- 1123 Barrows, T.T., Williams, M.A., Mills, S.C., Duller, G.A.T., Fifield, L.K., Haberlah, D., Tims, S.G.  
 1124 and Williams, F.M., 2014. A White Nile megalake during the last interglacial period.  
 1125 *Geology* 42, 163-166.
- 1126 Beudet, G., Coque, R., Michel, P., Rognon, P. 1977. Y-a-t-il eu captured Niger? *Bull. Ass.*  
 1127 *Geogr. Fr.* 445/446, 215-222.
- 1128 Bleicher N. 2013 Summed radiocarbon probability density functions cannot prove solar  
 1129 forcing of Central European lake-level changes. *Holocene* 23, 755-765.
- 1130 Bristow, C.S., Holmes, J.A., Matthey, D., Salzmann, U., Sloane, H. 2018 A late Holocene  
 1131 palaeoenvironmental “snapshot” of the Angamma Delta, Lake Megachad at the end  
 1132 of the African Humid Period. *Quat. Sci. Rev.* 202, 182-196.
- 1133 Bristow, C.S., Armitage, S.J. 2016 Dune ages in the sand deserts of the southern Sahara and  
 1134 Sahel. *Quat. Int.* 410, 46-57.
- 1135 Brooks, N., Drake, N., MacLaren, S., White, K., 2003. *Studies in Geography, Geomorphology,*  
 1136 *Environment and Climate.* In Mattingly, D. J. M., Dore, J. and Wilson, A. I. (Eds.) *The*  
 1137 *Archaeology of Fezzan Volume I: Synthesis.* Society for Libyan Studies, London, pp 37-  
 1138 74.
- 1139 Causse, C., G. Conrad, J. Ch. Fontes, F. Gasse, E. Gibert and A. Kassir, 1988. Le dernier  
 1140 ‘Humide’ plitistocene du Sahara nord-occidental daterait de 80-100000 ans. *C R Acad.*  
 1141 *Sci.* 306, II: 1459-1464.
- 1142 Causse, C., Coque, R., Fontes, Ch, J., Gasse, F., Gibert, E., Ben Ouezdou, H.B., Zouari, K., 1989.  
 1143 Two high levels of continental waters in the southern Tunisian chotts at about 90 and  
 1144 150 ka. *Geology* 17, 922-925.

- 1145 Causse, C., Ghaleb, B., Chkir, N., Zouari, K., Ouezdou, H.B. and Mamou, A., 2003. Humidity  
1146 changes in southern Tunisia during the Late Pleistocene inferred from U–Th dating of  
1147 mollusc shells. *Appl. Geochem.* 18, 1691-1703.
- 1148 Claussen, M., Dallmeyer, A., Bader, J., 2017. Theory and modelling of the African humid  
1149 period and the green Sahara. In: *Oxford Research Encyclopedia of Climate Science*.
- 1150 Conrad, G. 1970. L'évolution continentale post-hercynienne du Sahara algérien:(Saoura, Erg  
1151 Chech-Tanezrouft, Ahnet-Mouydir). Éditions du Centre national de la recherche  
1152 scientifique.
- 1153 Conrad, G., Lappartient, J.R., 1991. The appearance of *Cardium* fauna in the great lakes of  
1154 the early Quaternary period in the Algerian central Desert. *J. Afr. Earth Sci.* 12, 375–  
1155 382.
- 1156 Coque, R. 1962. *La Tunisie présaharienne*. Armand Colin, Paris.
- 1157 de Menocal, P. B., 2000. Abrupt onset and termination of the African Humid Period: Rapid  
1158 climate responses to gradual insolation forcing. *Quat. Sci. Rev.* 19, 347-361
- 1159 de Menocal, P. B., 2001. Cultural responses to climate change during the late Holocene.  
1160 *Science* 292, 667-673.
- 1161 Drake, N.A., 1997. Recent Aeolian origin of surficial gypsum crusts in southern Tunisia:  
1162 Geomorphological, archaeological and remote sensing evidence. *Earth Surf. Process.*  
1163 *Landf.* 22, 641-656.
- 1164 Drake, N.A. and Bristow, C. 2006. Shorelines in the Sahara: geomorphological evidence for an  
1165 enhanced monsoon from palaeolake Megachad. *Holocene* 16, 901-911.
- 1166 Drake, N.A. and Breeze, P. 2016. Climate Change and Modern Human Occupation of the  
1167 Saharan from MIS Stage Six to Two. In: Jones, S and Stewart, B. (Eds.) *Africa from MIS*  
1168 *6-2: Population Dynamics and Palaeoenvironments*. Springer Science+Business  
1169 Media, Dordrecht, pp 103-122.
- 1170 Drake, N.A., El-Hawat, A.S., Turner, P., Armitage S.J., Salem, M.J., White, K.H., McLaren S.  
1171 2008. Palaeohydrology of the Fazzan Basin and Surrounding Regions: the Last 7  
1172 Million Years. *Palaeogeogr. Palaeoclimatol. Palaeoecol.* 263, 131–145,

1173 Drake, N.A., Blench, R.M., Armitage, S.J., Bristow, C.S., White K.H. 2011. Ancient  
1174 watercourses and biogeography of the Sahara explain the peopling of the desert.  
1175 Proc. Natl. Acad. Sci. U S A 108, 458-462.

1176 Drake, N.A., Lem, R.E., Armitage, S.J., White K.H., El-Hawat A., Salem, M.J., Hounslow, M.,  
1177 2018. Reconstructing palaeoclimate and hydrological fluctuations in the Fezzan Basin  
1178 (southern Libya) since 130 ka: A catchment-based approach. Quat. Sci. Rev. 200, 376-  
1179 394.

1180 Dumont H.J. 1987. Sahara. In Burgis, M.J. and Symoens, J.J. (Eds.) *African wetlands and*  
1181 *shallow water bodies = Zones humides et lacs peu profonds d'Afrique.*

1182 El-Shenawy, M.I., Kim, S.T., Schwarcz, H.P., Asmerom, Y. and Polyak, V.J., 2018. Speleothem  
1183 evidence for the greening of the Sahara and its implications for the early human  
1184 dispersal out of sub-Saharan Africa. Quat. Sci. Rev. 188, 67-76.

1185 Fick, S.E. and Hijmans, R.J., 2017. WorldClim 2: new 1-km spatial resolution climate surfaces  
1186 for global land areas. Int. J. Climatol. 37(12), 4302-4315.

1187 Fischer, M.L., Markowska, M., Bachofer, F., Foerster, V., Asrat, A., Zielhofer, C., Trauth, M.H.  
1188 and Junginger, A., 2020. Determining the pace and magnitude of lake level changes in  
1189 southern Ethiopia over the last 20,000 years using Lake Balance Modelling and  
1190 SEBAL. Front. Earth Sci. 8, p.197.

1191 Foerster, V., Junginger, A., Langkamp, O., Gebru, T., Asrat, A., Umer, M., Lamb, H.F.,  
1192 Wennrich, V., Rethemeyer, J., Nowaczyk, N. and Trauth, M.H., 2012. Climatic change  
1193 recorded in the sediments of the Chew Bahir basin, southern Ethiopia, during the last  
1194 45,000 years. Quat. Int. 274, 25-37.

1195 Gasse, F. (2002), Diatom inferred salinity and carbonate oxygen isotopes in Holocene  
1196 waterbodies of the western Sahara and Sahel (Africa), Quat. Sci. Rev. 21, 737– 767.

1197 Geyh, M.A., Thiedig, F., 2008. The Middle Pleistocene Al Mahruqah Formation in the Murzuq  
1198 Basin, northern Sahara, Libya evidence for orbitally-forced humid episodes during the  
1199 last 500,000 years. Palaeogeogr. Palaeoclimatol. Palaeoecol. 257, 1–21.

- 1200 Ghoneim, E. and El-Baz, F., 2007. DEM-optical-radar data integration for palaeohydrological  
1201 mapping in the northern Darfur, Sudan: implication for groundwater exploration. *Int.*  
1202 *J. Remote Sens.* 28, 5001-5018.
- 1203 Grove, A.T., Warren, A., 1968. Quaternary landforms and climate on the south side of the  
1204 Sahara. *Geogr. J.* 134, 194-208.
- 1205 Goudie, A.S., 1992. *Environmental Change*. Oxford University Press, Oxford.
- 1206 Helmke, J.P., Bauch, B.A., Röhl, U., Kandiano, E.S., 2008. Uniform climate development  
1207 between the subtropical and subpolar Northeast Atlantic across marine isotope stage  
1208 11. *Clim. Past* 4, 433-457.
- 1209 Hill, C.L. and Schild, R., 2017. Pleistocene deposits in the Southern Egyptian Sahara:  
1210 lithostratigraphic relationships of sediments and landscape dynamics at Bir  
1211 Tarfawi. *Studia Quat.* 34, 23-38.
- 1212 Hoelzmann, P., Keding, B., Berke, H., Kröpelin, S. and Kruse, H.J., 2001. Environmental  
1213 change and archaeology: lake evolution and human occupation in the Eastern Sahara  
1214 during the Holocene. *Palaeogeogr. Palaeoclimatol. Palaeoecol.* 169, 193-217.
- 1215 Hoelzmann, P., Kruse, H.J. and Rottinger, F., 2000. Precipitation estimates for the eastern  
1216 Saharan palaeomonsoon based on a water balance model of the West Nubian  
1217 Palaeolake Basin. *Glob. Planet. Change* 26, 105-120.
- 1218 Hopcroft, P.O., Valdes, P.J., Harper, A.B. and Beerling, D.J., 2017. Multi vegetation model  
1219 evaluation of the Green Sahara climate regime. *Geophys. Res. Lett.* 44, 6804-  
1220 6813.
- 1221 Hounslow, M., White, H., Drake, N.A., Salem, M.J., El-Hawat A., McLaren, S.J., Karloukovski,  
1222 V., Hlal O. 2017. Miocene humid intervals and establishment of drainage networks by  
1223 23 Ma in the central Sahara, southern Libya. *Gondwana Res.* 45, 118-137.
- 1224 Jousse, H., Obermaier, Raimbault, M. and Peter, J. 2008. Late Holocene Economic  
1225 Specialisation Through Aquatic Resource Exploitation at Kobadi in the Méma, Mali.  
1226 *Int. J. Osteoarchaeol* 18, 549-572.



- 1227 Kropelin, S., Verschuren, D., Lezine, A.-M., Eggermont, H., Coquyt, C., Francus, P., Cazet, J.-P.,  
1228 2008. Climate-driven ecosystem succession in the Sahara: the past 6000 years.  
1229 Science 320, 765-768.
- 1230 Kuper, R., Kropelin, S., 2006. Climate-controlled Holocene occupation of the Sahara: motor  
1231 of Africa's evolution. Science 313, 803-807.
- 1232 Kutzbach, J.E., Street-Perrot, F.A., 1985. Milankovitch forcing of fluctuations in the level of  
1233 tropical lakes from 18-0 k yr BP. Nature 317, 1301-34.
- 1234 Lehner, B., Verdin, K., Jarvis, A., 2008. New global hydrography derived from spaceborne  
1235 elevation data. Eos Trans. AGU 89, 93-94.
- 1236 Maxwell, T.A., Issawi, B. and Haynes Jr, C.V., 2010. Evidence for Pleistocene lakes in the  
1237 Tushka region, south Egypt. Geology 38, 1135-1138.
- 1238 Meckler, A.N., Clarkson, M.O., Cobb, K.M., Sodemann, H., Adkins, J.F., 2012. Interglacial  
1239 Hydroclimate in the Tropical West Pacific Through the Late Pleistocene.  
1240 Scienceexpress ([http://www.sciencemag.org/content/early/recent/3 May](http://www.sciencemag.org/content/early/recent/3%20May%202012/10.1126/science.1218340)  
1241 2012/10.1126/science.1218340).
- 1242 Pachur, H.J., Rottinger, F., 1997. Evidence for a large extended paleolake in the eastern  
1243 Sahara as revealed by space borne radar lab images. Remote Sens. Environ. 61, 437-  
1244 440.
- 1245 Pekel, J.-F., Cottam, A., Gorelick, N., Belward, A.S., 2016. High-resolution mapping of global  
1246 surface water and its long-term changes. Nature 540, 418-422.
- 1247 Petit-Maire, N., Riser, J. 1987. Holocene palaeohydrography of the Niger. Paleoecol. Afr. 18,  
1248 135-141.
- 1249 Petit-Maire, N., Celles, J.C., Commelin, D., Delibrias, G. and Raimbault, M. 1983. The Sahara  
1250 in Northern Mali: Man and His Environment between 10,000 and 3500 Years bp.  
1251 (Preliminary Results). Afr. Archaeol. Rev. 1, 105-125.
- 1252 Prell, W.L., Kutzbach, J.E. 1987. Monsoon variability over the past 150,000 years. J. Geophys.  
1253 Res. 92, D7, 8411-8425.

- 1254 Pruszek, Z., Rozynski, G. and Szmytkiewicz, P. 2008. Megascale rhythmic shoreline forms on a  
1255 beach with multiple bars. *Oceanologia* 50, 183-203.
- 1256 Quade, J., Dente, E., Armon, M., Ben Dor, Y., Morin, E., Adam, O., Enzel, Y., Megalakes in the  
1257 Sahara? A Review. *Quat. Res.* 90, 253-275.
- 1258 Raimbault, M., 1986. Le gisement Néolithique de Kobadi (Sahel Malien) et ses implications  
1259 paléohydrologiques. In Faure, H., Faure, L., & Diop, E.S. (eds.). *Changements*  
1260 *Globaux en Afrique durant le Quaternaire: Passe, Present, Futur.* Orstom, Paris, 393-  
1261 397.
- 1262 Reineck, H.E., Singh, I.R., 1980. *Depositional Sedimentary Environments.* Springer-Verlag,  
1263 Berlin, pp 548.
- 1264 Richards, G.W., Vita-Finzi, C., 1982. Marine deposits 35,000-25,000 years old in the Chott el  
1265 Djerid, southern Tunisia. *Nature* 294, 54-55.
- 1266 Riser, J., Hillaire-Marcel, C., Rognon, P. 1984. Les phases lacustres Holocènes. In Petit-Maire,  
1267 N. & Riser, J. (Eds) *Sahara Ou Sahel? Quaternaire Récent du Bassin de Taoudenni*  
1268 *(Mali).* Laboratoire de Géologie du Quaternaire du CNRS, pp. 65-84.
- 1269 Roberts, C.R. and Mitchell, C.W., 1987. Spring mounds in southern Tunisia. *Geol. Soc. Spec.*  
1270 *Publ.* 35 (1), 321-334. Schuster, M., Roquin, C., Durringer, P., Brunet, M., Caugy, M.,  
1271 Fontugne, M., Mackaye, H.T., Vignaud, P. and Ghienne, J.F., 2005. Holocene lake  
1272 Mega-Chad palaeoshorelines from space. *Quat. Sci. Rev.* 24, 1821-1827.
- 1273 Servant, M. and Servant, S., 1983. Paleolimnology of an upper quaternary endorheic lake in  
1274 Chad basin. In: Servant, M. and Servant, S. (Eds.) *Lake Chad.* Springer, Dordrecht, pp  
1275 11-26.
- 1276 Shennan, S., Downey, S.S., Timpson, A., Edinborough, K., Colledge, S., Kerig, T., Manning K.,  
1277 Thomas. M.G. 2013. Regional population collapse followed initial agriculture booms  
1278 in mid-Holocene Europe. *Nat. Commun.* 4, 1-8.
- 1279 Surovell T.A., Finley, J.B., Smith, G.M., Brantingham, P.J., Kelly, R. 2009 Correcting temporal  
1280 frequency distributions for taphonomic bias. *J. Archaeol. Sci.* 36, 1715-1724.

- 1281 Swezey, C.S., 2003. The role of climate in the creation and destruction of continental  
1282 stratigraphic records: an example from the northern margin of the Sahara Desert.  
1283 SEPM Special Publication 77.
- 1284 Szabo, B.J., Haynes Jr, C.V. and Maxwell, T.A., 1995. Ages of Quaternary pluvial episodes  
1285 determined by uranium-series and radiocarbon dating of lacustrine deposits of  
1286 Eastern Sahara. *Palaeogeogr. Palaeoclimatol. Palaeoecol.* 113, 227-242.
- 1287 Thiedig, F.M., Oezen, D., El-Chair, M., Geyh, M.A., 2000. The absolute age of the Quaternary  
1288 lacustrine limestone of the Al Mahruqah Formation — Murzuq Basin, Libya. In: Sola,  
1289 M.A., Worsley, D. (Eds.), *Geological Exploration in the Murzuq Basin*. Elsevier,  
1290 Amsterdam, pp. 89–116.
- 1291 Vaks, A., et al., 2010. Middle-Late Quaternary palaeoclimate of northern margins of the  
1292 Saharan-Arabian Desert: reconstruction from speleothem of Negev Desert, Israel.  
1293 *Quat. Sci. Rev.* 29, 2647-2662.
- 1294 Van Neer, W. 2012. Fish remains from the late glacial at Bir Tarfawi. In: Close, A.E., Schild, R.  
1295 and Wendorf, F., *Egypt During the Last Interglacial: The Middle Paleolithic of Bir*  
1296 *Tarfawi and Bir Sahara East*. Springer Science & Business Media, pp 144-155.
- 1297 Vernet, R. 1998. Le Sahara et le Sahel. Paléoenvironnements et occupation humaine à la fin  
1298 du pléistocène et à l'Holocène. *Inventaire des Datations 14C*. Université Nouakchott,  
1299 Cria, 147Pp.
- 1300 Walker, M.J.C. 2005. *Quaternary Dating Methods*. J Wiley and Sons.
- 1301 Walton Jr, T.L., 1999. Shoreline rhythmic pattern analysis. *J. Coast. Res.* 379-387.
- 1302 Washington, R., Todd, M.C., Lizcano, G., Tegen, I., Flamant, C., Koren, I., Ginoux, P.,  
1303 Engelstaedter, S., Bristow, C.S., Zender, C.S., Goudie, A.S., Warren, A., Prospero, J.M.,  
1304 2006. Links between topography, wind, deflation, lakes and dust: The case of the  
1305 Bodélé Depression, Chad. *Geophys. Res. Lett.* 33.
- 1306 Williams, M.A., Adamson, D., Prescott, J.R. and Williams, F.M., 2003. New light on the age of  
1307 the White Nile. *Geology* 31, 1001-1004.

- 1308 Williams, M., Talbot, M., Aharon, P., Abdl Salaam, Y., Williams, F., and Inge Brendeland, K.,  
1309 2006, Abrupt return of the summer monsoon 15,000 years ago: new supporting  
1310 evidence from the lower White Nile valley and Lake Albert: *Quat. Sci. Rev.* 25, 2651-  
1311 2665.
- 1312 Zielhofer, C., Fletcher, W.J., Mischke, S., De Batist, M., Campbell, J.F., Joannin, S., Tjallingii, R.,  
1313 El Hamouti, N., Junginger, A., Stele, A. and Bussmann, J., 2017. Atlantic forcing of  
1314 Western Mediterranean winter rain minima during the last 12,000 years. *Quat. Sci.*  
1315 *Rev.* 157, 29-51.
- 1316 Zouari, K., Chkir, N., Causse, C., 1998. Pleistocene humid episodes in southern Tunisian  
1317 Chotts. In: *Isotope techniques in the study of environmental change. Proceedings of*  
1318 *an International Symposium, Vienna, April 14-18, 1997. IAEA-SM-349/41, pp. 543-*  
1319 *554.*
- 1320